

A Sillimanite Gneiss Dome in
the Yukon Crystalline Terrane,
East-Central Alaska:
Petrography and Garnet-
Biotite Geothermometry

GEOLOGICAL SURVEY PROFESSIONAL PAPER 1170-E



A Sillimanite Gneiss Dome in the Yukon Crystalline Terrane, East-Central Alaska: Petrography and Garnet- Biotite Geothermometry

By CYNTHIA DUSEL-BACON *and* HELEN L. FOSTER

SHORTER CONTRIBUTIONS TO GENERAL GEOLOGY

GEOLOGICAL SURVEY PROFESSIONAL PAPER 1170-E

*Petrographic, geothermometric, and structural data are used
to support the hypothesis that a 600-km² area of
pelitic metamorphic rocks is a gneiss dome*



UNITED STATES DEPARTMENT OF THE INTERIOR

JAMES G. WATT, *Secretary*

GEOLOGICAL SURVEY

Dallas L. Peck, *Director*

Library of Congress Cataloging in Publication Data

Dusel-Bacon, Cynthia.

A sillimanite gneiss dome in the Yukon crystalline terrane, east-central Alaska.

(Shorter contributions to general geology) (Geological Survey Professional Paper 1170-E)

Bibliography

Supt. of Docs. no.: I 19.4/2:1170-E

1. Gneiss—Alaska. 2. Intrusions (Geology)—Alaska. I. Foster, Helen Laura, 1919— . II. Title. III. Series. IV. Series:
United States: Geological Survey. Professional Paper 1170-E.

QE475.G55D87 1983

552'.4

83-600031

**For sale by the Distribution Branch, U.S. Geological Survey,
604 South Pickett Street, Alexandria, VA 22304**

CONTENTS

	Page
Abstract.....	E1
Introduction.....	1
Acknowledgments.....	2
Geologic setting.....	2
Field relations and macroscopic characteristics of the sillimanite gneiss and associated pelitic schist.....	3
Petrographic description of the aluminum-silicate-bearing rocks of the Salcha River area	6
Sillimanite gneiss.....	6
Equigranular feldspathic rocks.....	10
Pelitic schist.....	10
Geothermometry based on coexisting garnet and biotite in the pelitic schist and sillimanite gneiss.....	14
Discussion.....	17
Metamorphic reactions and isograds in pelitic schist and sillimanite gneiss.....	17
Staurolite+biotite isograd.....	17
Staurolite-out isograd.....	20
Sillimanite-andalusite isograd.....	21
Proposed origin of equigranular aluminum-silicate-bearing rocks.....	21
Physical conditions of metamorphism.....	21
Conclusions.....	23
References cited.....	23

ILLUSTRATIONS

	Page
FIGURE 1. Index map showing location of study area in east-central Alaska.....	E2
2. Geologic map of the sillimanite gneiss and vicinity showing distribution of key minerals and metamorphic isograds.....	4
3. Photograph showing marble nodule in sillimanite gneiss.....	5
4. Photograph showing contact between granitic rock and sillimanite-biotite gneiss.....	6
5. Photomicrographs showing textural relations in sillimanite gneiss, equigranular feldspathic rock, and pelitic schist.....	11
6. Simplified geologic map of pelitic schist and sillimanite gneiss showing location of garnet-biotite samples.....	19
7. Diagram showing phase equilibria pertaining to study area.....	22

TABLES

	Page
TABLE 1. Major-element data and CIPW norms for samples of sillimanite gneiss.....	E6
2. Representative mineral assemblages of aluminum-silicate-bearing rocks.....	8
3. Representative chemical analyses of biotite.....	15
4. Representative chemical analyses of garnet.....	16
5. Distribution coefficients for the Fe/Mg ratio in coexisting garnet and biotite and equilibration temperatures (in degrees Celsius) calculated at 0.4-GPa total pressure.....	18

SHORTER CONTRIBUTIONS TO GENERAL GEOLOGY

**A SILLIMANITE GNEISS DOME IN THE
YUKON CRYSTALLINE TERRANE, EAST-CENTRAL ALASKA:
PETROGRAPHY AND GARNET-BIOTITE GEOTHERMOMETRY**

By CYNTHIA DUSEL-BACON and HELEN L. FOSTER

ABSTRACT

A topographically high, nearly circular area of sillimanite gneiss crops out over approximately 600 km² in the Big Delta quadrangle, Yukon crystalline terrane, east-central Alaska. Foliation is generally horizontal or subhorizontal in the center of the gneiss body and dips outward in all directions. Felsic dikes, some of which are pegmatitic, occur in the central area of gneiss. Quartzite and marble are locally infolded in the gneiss, particularly near its margins. The gneiss is partly bordered on the north and east by pelitic schist interlayered with lesser amounts of quartzite, marble, and amphibole schist. The ages of the protoliths of these rocks are believed to be Paleozoic or possibly Precambrian; major metamorphism probably took place between Mississippian and Middle Triassic time. Two isograds within the pelitic schist are concentric to the gneiss body and indicate an increase in metamorphic grade toward the gneiss. The outermost isograd is defined by the appearance of staurolite with biotite, at the expense of chlorite and muscovite. Upgrade of this isograd, several combinations of the aluminum silicate polymorphs (andalusite, kyanite, and sillimanite) +garnet+staurolite are present in quartz-biotite-muscovite schist. Textural relations suggest that these three polymorphs all formed during the same prograde metamorphic event in which pressure-temperature conditions were near the triple point. The innermost isograd, defined by the disappearance of staurolite, closely coincides with the schist-gneiss contact. Increase in metamorphic grade in the gneiss (quartz+biotite+sillimanite+orthoclase+plagioclase± muscovite± garnet and locally quartz+biotite+sillimanite+cordierite+orthoclase +plagioclase +muscovite) is indicated by an increase in modal orthoclase and decrease in muscovite toward the center of the body, consistent with the breakdown of muscovite+quartz. Migmatitic textures, although rare, may be evidence of local partial melting of the gneiss. The relative distribution of Fe and Mg between garnet and biotite indicates equilibration at about 535° to 600°±30°C for pelitic schist north of the gneiss body and 655° to 705°±30°C for sillimanite gneiss. Petrographic data from poorly exposed rocks south and west of the gneiss also suggest an increase in pressure and (or) temperature conditions toward the gneiss body; such an increase is indicated by an isograd which separates andalusite-sillimanite-bearing schist and gneiss to the southwest from sillimanite gneiss to the northeast. Evidence that the sillimanite gneiss is a dome consists of: (1) the topographic expression and radial drainage pattern, (2) the outward dip of foliation, (3) an increase in metamorphic grade toward the center of the body, and (4) an increase in garnet-biotite temperatures inward. Minor intrusion of synmetamorphic dikes or small granitic bodies is suggested by the presence of equigranular, aluminum-silicate-bearing rocks at several localities in the proposed dome which contain textural

features indicative of both igneous and metamorphic processes. The staurolite-out and andalusite-sillimanite isograds define the northern and eastern and the southwestern margins, respectively, of the proposed gneiss dome.

INTRODUCTION

Sillimanite gneiss crops out in a 600 km² area in the central part of the Big Delta quadrangle, east-central Alaska, near the northwestern margin of the Yukon crystalline terrane (fig. 1). On an early geologic map of the Yukon-Tanana region (Mertie, 1937), the gneiss and most of the surrounding schists were included in a single geologic unit, the Birch Creek Schist (of former usage). The general geology of the area is shown at a scale of 1:63,360 on a reconnaissance geologic map by Foster and others (1977a) and at a scale of 1:250,000 on a reconnaissance geologic map (Weber and others, 1978). The possibility that the area of sillimanite gneiss might be a gneiss dome was reported initially by Foster and others (1977b).

In this paper we present new petrographic and petrologic data on the sillimanite gneiss and surrounding pelitic schist, and we interpret these data in terms of the metamorphic history of these rocks. In particular, we address the hypothesis that the large, topographically high area of sillimanite gneiss is a gneiss dome. This is the first gneiss dome in the Yukon crystalline terrane to be reported in the literature, but reconnaissance mapping in the Alaskan part of the crystalline terrane (Weber and others, 1978) has identified other areas of gneiss which appear roughly circular in plan view and which also may prove to be gneiss domes.

This particular body of sillimanite gneiss, flanked by pelitic schist, was chosen for study because of the abundance of mineral assemblages containing the pressure-temperature-sensitive aluminum silicates and the relatively good exposure of the gneiss. The distribution of aluminum silicates in thin sections of

pelitic schist and sillimanite gneiss enables the estimation of metamorphic pressure and temperature conditions, and garnet-biotite pairs in these same rocks provide an additional means of determining metamorphic temperatures. Because kyanite, andalusite, and sillimanite occur together in single thin sections of pelitic schist from four different localities, we also have attempted to determine whether or not these Al_2SiO_5 polymorphs crystallized during a single metamorphic episode and thus whether their occurrence indicates triple-point conditions in the schist. Study of the sillimanite gneiss dome can provide a basis for subsequent comparisons with other such structures in Alaska and the Canadian Cordillera.

This paper is an outgrowth of geologic mapping of the Big Delta quadrangle for the U.S. Geological Survey's Alaska Mineral Resource Assessment Program (Foster and others, 1979). Most of the fieldwork, all of which was of a reconnaissance nature, was done in 1976 and 1977; the laboratory work was accomplished mainly in 1979 and 1980.

ACKNOWLEDGMENTS

We wish especially to recognize the many contributions of Florence R. Weber to the mapping of the Big Delta quadrangle and her initial recognition of sillimanite gneiss in the area. We are also indebted to Charles R. Bacon for microprobe analyses, aid in interpretation of the data, and support throughout the study. Discussions of metamorphic petrology and petrography with Jo Laird and Anna Hietanen have been particularly valuable.

GEOLOGIC SETTING

The sillimanite gneiss occurs in the Yukon crystalline terrane (Tempelman-Kluit, 1976), a geologically complex metamorphic and igneous terrane that is bounded by two major right-lateral strike-slip fault systems, the Tintina to the north and the Denali to the south (fig. 1). Tempelman-Kluit (1976) has proposed that much of this terrane is allochthonous, and

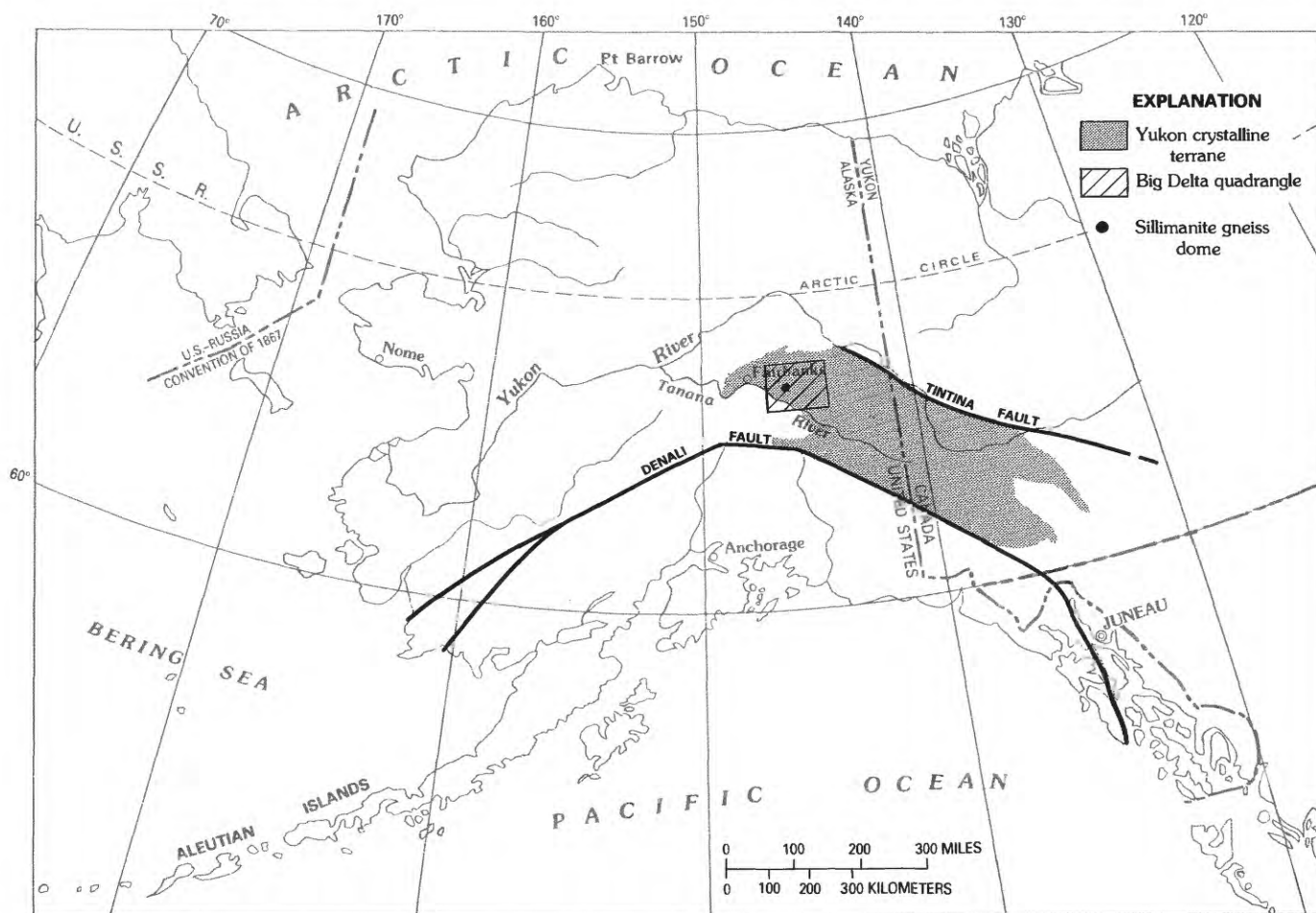


FIGURE 1.—Location of sillimanite gneiss dome, Yukon crystalline terrane, and Big Delta quadrangle in east-central Alaska.

according to Foster and Keith (1974), it is possibly a continental fragment that moved in over oceanic crust along an ancient suture bordering the North American plate. Churkin and others (1982) suggest that the terrane may be composed of at least four subterraneans.

The metamorphic rocks of the Yukon crystalline terrane range in metamorphic grade from low greenschist to amphibolite facies. They have been intruded by Mesozoic and Tertiary granitic plutons, and small areas are overlain by Mesozoic and Tertiary volcanic and sedimentary rocks. Several masses of ultramafic rocks, including alpine-type serpentized peridotite and dismembered ophiolite assemblages, have been tectonically emplaced.

Most of the metamorphic rocks are derived from protoliths with continental affinities, although some greenstones and other volcanic and ultramafic rocks occur which have oceanic, mantle, or island-arc affinities. Quartzitic rocks are most abundant, but there are also interlayered marble, pelite, calc-silicate rocks, and mafic schist. Although pelitic gneiss and schist are not generally abundant in much of the Yukon crystalline terrane, in the central part of the Big Delta quadrangle such rocks occupy a significant area, including the region discussed in this paper. Lesser amounts of pelitic rocks occur in other parts of this quadrangle and in the Circle quadrangle to the north. Metagneous rocks, particularly ortho-augen gneiss (Aleinikoff and others, 1981), crop out, but in most areas are subordinate to metasedimentary rocks. Areas of augen gneiss (Weber and others, 1978; Foster, 1970, 1976; Tempelman-Kluit and Wanless, 1980; and J. K. Mortensen, written commun., 1982) that probably represent deformed batholiths define a crude northwesterly-trending belt across the Yukon crystalline terrane.

The ages of the protoliths are poorly known because of the lack of fossils, the scarcity of radiometric age data, and the difficulty of interpreting those data. Much of the metamorphic terrane is believed to have Paleozoic protoliths but Precambrian protoliths may also be present (Foster, 1976). Although the presence of Precambrian protoliths is uncertain, some rocks contain detrital material of Proterozoic age as indicated by U-Pb data for zircon separates from quartzites (Aleinikoff and others, 1983b).

The timing and number of metamorphic events that have affected various parts of the terrane are uncertain. In Alaska, or at least that part of it in which the sillimanite gneiss body occurs, the presence of an unmetamorphosed granitic pluton of Triassic age, about 210 m.y. old (Aleinikoff and others, 1981a), that intrudes the terrane and contains xenoliths of

metamorphic rocks suggests that major metamorphism of the terrane may have occurred before Middle Triassic time. Radiometric dating of a deformed batholith of augen gneiss (Aleinikoff and others, 1981b) that crops out about 50 km southeast of the sillimanite gneiss indicates that major metamorphism occurred either during or after the intrusion of the augen gneiss protolith in Early Mississippian time. Recent U-Pb dating of zircons from the sillimanite gneiss described in this paper (Aleinikoff and others, 1983a) has yielded results that could be interpreted to indicate that metamorphism of the sillimanite gneiss was roughly synchronous with Mississippian intrusion of the augen gneiss. The U-Pb zircon ages also indicate an early Proterozoic provenance age (2.0 to 2.3 b.y.) for the sedimentary protolith of the sillimanite gneiss.

FIELD RELATIONS AND MACROSCOPIC CHARACTERISTICS OF THE SILLIMANITE GNEISS AND ASSOCIATED PELITIC SCHIST

The sillimanite gneiss occurs in a topographically high, nearly circular area south of the Salcha River (fig. 2). Maximum relief in this area is about 1,200 m, and drainage is outward in all directions from the center of the gneiss body. Exposure of the gneiss is fairly good above the tree and brush line, which is about 1,000 m in elevation. Altiplanation terraces and patterned ground are well developed on high ridges, and coarse frost-riven rock rubble generally covers the surface; outcrops are scattered widely. Foliation, defined by the alinement of biotite flakes and elongate quartz grains, is moderately to poorly developed and is characteristically nearly horizontal in the central part of the area of gneiss. The nearly horizontal attitudes result from recumbent isoclinal folding on both a mesoscopic and macroscopic scale. Dips of foliation are roughly outward in all directions from the center of the gneissic area and are rarely more than 30°. The few attainable measurements of fold axes indicate that they have a general westerly strike with no consistent direction of plunge. Diopside-bearing marble and quartzite, once interlayered with the pelitic rocks, now occur only locally as discontinuous layers and blocks in the sillimanite gneiss (fig. 3). Brittle, cataclastic deformation of the gneiss has also occurred, but its effects are not so readily visible in the field as are those of ductile deformation. The gneiss is faulted in places (fig. 2), but faults are not mapped in detail.

The rocks throughout the sillimanite gneiss body are much alike in mineral composition and texture. Major-element analyses and norms for two samples of

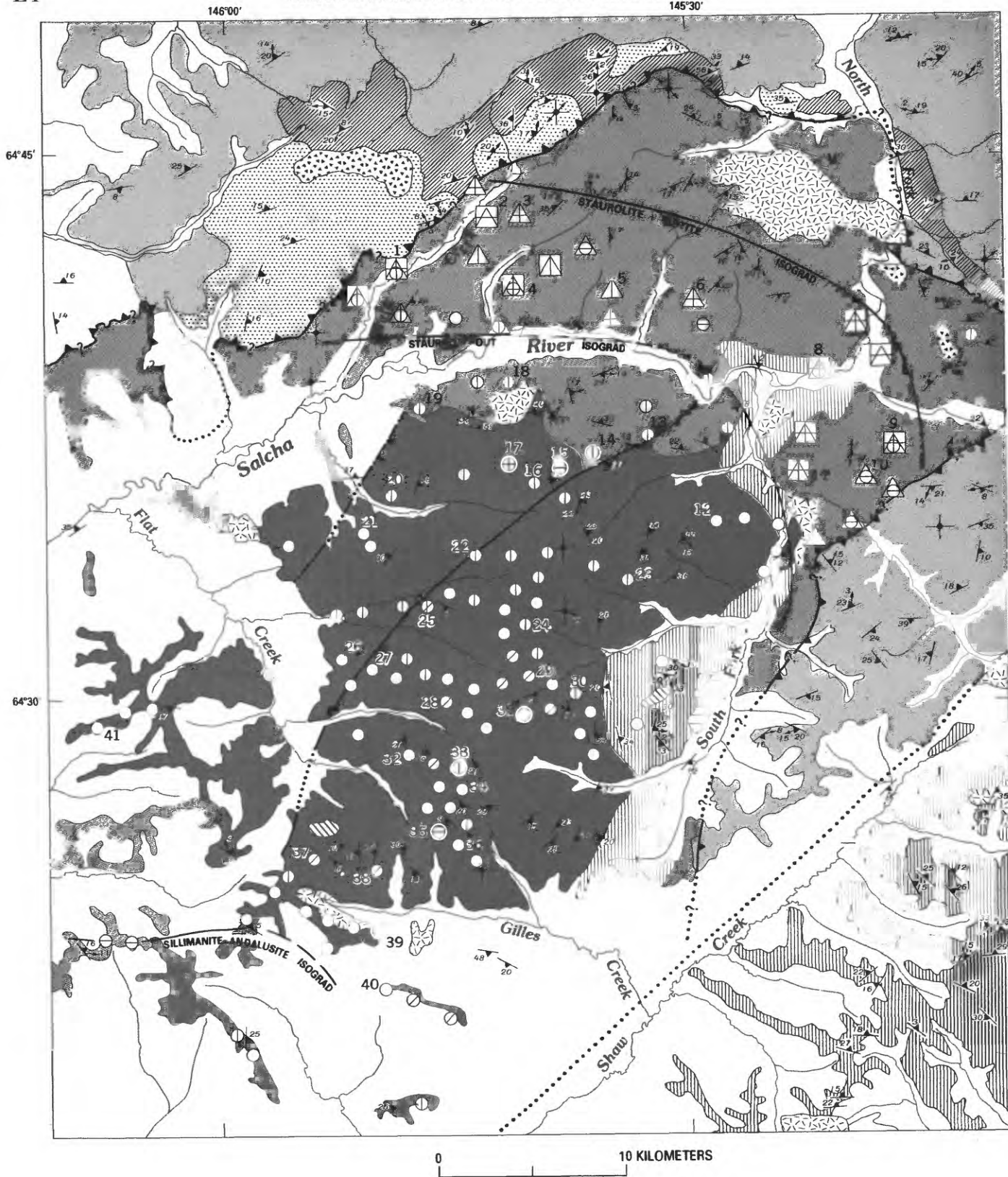



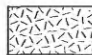









FIGURE 2.—Geologic map of the sillimanite gneiss body and vicinity (after Weber and others, 1978) showing distribution of key minerals and metamorphic isograds.

sillimanite gneiss that are representative of the gneiss body are shown in table 1. Chemical compositions of these rocks are compatible with the sedimentary pro-

tolith proposed for the gneiss: that is, K is greater than Na and Mg greater than Ca; also, normative quartz is close to or greater than the 50-percent value considered by Mason (1966, p. 249) to be indicative of a sedimentary protolith. The gneiss is medium dark brown in color and fine to medium grained. Biotite, quartz, orthoclase, and plagioclase generally occur as scattered subequant grains that average a millimeter in size and give the rock a characteristic "salt and pepper" appearance. The sillimanite is rarely coarse enough to be seen with a hand lens, but where visible it appears as fine, milky-white threads. Because of the subequant shape of biotite flakes and a lack of pronounced mineral segregation, gneissic banding is commonly poorly defined. Biotite-rich layers and clots of biotite occur locally, and swirly banding is particularly evident in the biotite-rich layers. Migmatitic streaking, suggested by textural and compositional differences on the order of a few centimeters, was observed at a few areas well within the gneiss body.

Unfoliated granitic-appearing rock, generally found only as rubble, is present in several areas in the central part of the gneiss body. The equigranular texture of the gneiss in these places makes it difficult to distinguish igneous from metamorphic textures. At a few localities, granitic rock and sillimanite-biotite

EXPLANATION

	SURFICIAL DEPOSITS—Alluvium, colluvium, loess, and sand	} QUATERNARY
	GRANITIC ROCKS—Granodiorite to quartz monzonite	
GREENSCHIST-FACIES ROCKS—As mapped, divided into:		} PERMIAN
	Peridotite, greenstone	
	Cataclastic quartzofeldspathic rocks	} PALEOZOIC(?)
	Semischist, greenschist, quartzite, and marble	
	Carbonaceous quartzite, argillite, marble and calc-phylite	
EPIDOTE-AMPHIBOLITE AND AMPHIBOLITE-FACIES ROCKS—As mapped, divided into:		} PALEOZOIC
	Metamorphosed diorite	
	Pelitic schist, quartzite, amphibole schist, and marble	} PALEOZOIC AND (OR) PRECAMBRIAN
	Sillimanite gneiss	
	Orthogneiss and paragneiss (includes biotite gneiss, amphibole gneiss, augen gneiss, and quartzite)	
	Metamorphosed peridotite and diorite	

*Note: Age relations between metamorphic units are unknown. Ages given here for metamorphic rocks are protolithic ages. Metamorphic ages for these rocks are uncertain but major metamorphism is probably post-earliest Mississippian to pre-Middle Triassic.



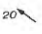

- Contact
- Fault—Dotted where concealed
- ▲ ? ▲ Probable thrust fault—Sawteeth on upper plate
- ····· Lineament observed on aerial photographs—Probable fault. Dotted where concealed
- Strike and dip of foliation
 -  Inclined
 -  Horizontal
- Bearing and plunge of fold axis or mineral lineation
 -  Inclined
 -  Horizontal
- Key minerals—Symbols may be combined; numbered locations refer to table 2 and figure 5A-L
 - Sillimanite
 - Kyanite
 - Andalusite
 - △ Staurolite
 - | Garnet, shown only where it occurs with one of the minerals above
 - / Cordierite
 - ⊙ Sillimanite-bearing equigranular feldspathic rock (may also contain other key minerals)



FIGURE 3.—Marble nodule (above hammer) in sillimanite gneiss from north-central part of gneiss body. Subhorizontal and horizontal foliation and recumbent folds are indicated by fracture pattern and subtle banding on weathered, lichen-covered outcrop.

TABLE 1.—Major-element data and CIPW norms for samples of sillimanite gneiss

Major elements (weight percent)		
	81ADB35A	81ADB36A
SiO ₂ -----	69.3	79.0
Al ₂ O ₃ -----	14.9	9.65
^b Fe ₂ O ₃ -----	6.21	3.43
MgO-----	2.18	1.20
CaO-----	.41	.84
Na ₂ O-----	.66	1.02
K ₂ O-----	3.53	2.89
TiO ₂ -----	.76	.52
P ₂ O ₅ -----	.05	.07
MnO-----	.06	.04
^c LoI-----	1.58	.81
Total-----	99.64	99.47

Norms (weight percent)		
	81ADB35A	81ADB36A
Q-----	49.02	59.48
Ab-----	5.71	8.76
An-----	1.75	3.76
Or-----	21.32	17.33
C-----	9.58	3.54
Fs-----	---	---
En-----	5.55	3.03
Ap-----	.12	.17
Il-----	1.48	1.00
Mt-----	4.08	1.97
Hm-----	1.41	.96

^aDetermined by quantitative X-ray spectroscopy.

^bTotal iron as Fe₂O₃.

^cLoss on ignition.

^dCalculated on the basis of Fe³⁺=2 Fe²⁺.

gneiss have a diffuse, irregular contact in outcrop; the granite may represent leucosomes in migmatitic gneiss (fig. 4) from synmetamorphic injection of the igneous material (to be discussed below). Felsic dikes and quartzofeldspathic, tourmaline-bearing pegmatite dikes cut the gneiss locally, particularly in the central area of gneiss. Potassium feldspar content in the gneiss is high in areas where these felsic dikes or granitic rocks occur. Xenoliths of biotite gneiss, marble, and quartzite (several centimeters to a meter in size) are partially assimilated in felsic and granitic dikes in the east-central part of the sillimanite gneiss body.

Toward the northern margin of the gneiss, a gradual increase in muscovite content is accompanied by a decrease in feldspar. Micaceous schist and fine-grained gneiss are interlayered just south of the Salcha River. North of the Salcha River the pelitic rocks are nearly all schistose and are interlayered with quartzitic schist, quartzite, marble, amphibole-bearing schist, and quartzofeldspathic schist.

Foliation in the schist generally dips an average of about 20° in an easterly direction. Lineation is formed by crenulation of the foliation, commonly seen in micaceous layers, and mineral alignment is somewhat inconsistent in trend and plunge but most commonly is oriented within 20° of north and plunges less than 5° to the north or south. Schists are only well exposed along crests of ridges and in scattered outcrops along the Salcha River and its tributaries.

Quartz-biotite-muscovite schist, commonly containing pink garnets up to a centimeter in diameter, is the most common rock type north of the Salcha River. Also present in many layers in the schist are dark-blue-gray andalusite porphyroblasts 1 or 2 cm long and small porphyroblasts, generally less than half a centimeter long, of dark-brown staurolite, black tourmaline, and dark-silvery-blue kyanite. Sillimanite, present in trace amounts in many schist samples, is too small to be detected in hand specimen.

The eastern margin of the sillimanite gneiss is the most complex, and it is bordered by a feldspathic gneiss interlayered with marble and amphibole-bearing biotite gneiss. These bordering rocks are mapped as a separate geologic unit, although they may be a part of the gneiss body. A small, foliated, Paleozoic diorite plug occurs west of the headwaters of the South Fork of the Salcha River (fig. 2). Several kilometers east of the plug, a small serpentinite mass apparently is infolded in feldspathic gneiss. East of the South Fork of the Salcha River, the sillimanite gneiss or other gneissic rocks grade into pelitic schist whose mineralogy and structures are similar to those on the north side of the sillimanite gneiss body. The

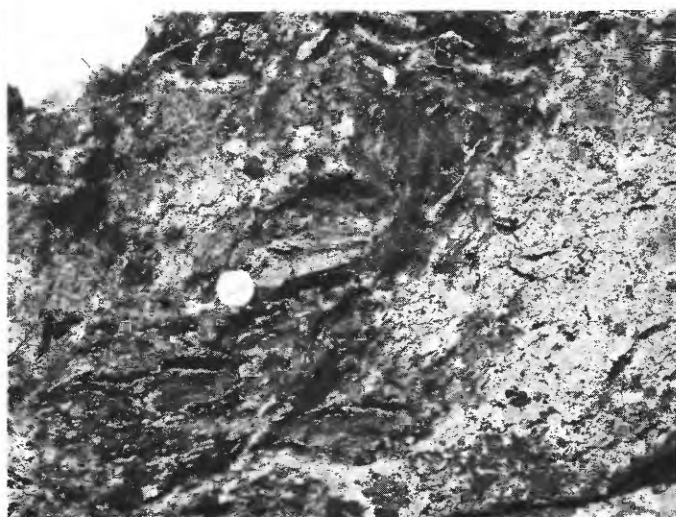


FIGURE 4.—Irregular, interfingering contact between granitic rock (right) and sillimanite-biotite gneiss from south-central part of gneiss body.

extent of the gneiss on the west and south is poorly known because the area is largely covered by loess, alluvium, sand, brush, and trees, but sillimanite-bearing rocks are known to occur as much as 40 km southwest of Gilles Creek (fig. 2).

North and east of the pelitic schist unit are greenschist facies rocks (Weber and others, 1978) that consist predominantly of quartzofeldspathic cataclastic rock, semischist, greenschist, quartzite, and marble (fig. 2). These greenschist facies rocks are probably in thrust contact with higher grade rocks which flank the sillimanite gneiss. A thrust is suggested by the zone of intensely cataclastic quartzofeldspathic rock north of the schist (fig. 2) and mylonitic textures in greenschist facies rocks east of the pelitic schist unit, apparent termination of isograds, and abrupt changes in lithology.

A few Cretaceous or Tertiary, unfoliated felsic plutons crop out in the area surrounding the gneiss (fig. 2). No contact metamorphic aureoles have been observed around these plutons. Incipient granoblastic texture and sericitization of white mica, noted in several thin sections from rocks near the large pluton west of the North Fork of the Salcha River, suggest that only minor thermal metamorphism has resulted locally.

PETROGRAPHIC DESCRIPTION OF THE ALUMINUM-SILICATE-BEARING ROCKS OF THE SALCHA RIVER AREA

Petrographic data for the aluminum-silicate-bearing lithologies—sillimanite gneiss, equigranular feldspathic rock, and pelitic schist—which occur in the Salcha River area are given in table 2, and sample locations are shown in figure 2. Only petrographic data for selected samples of sillimanite gneiss and pelitic schist that are considered representative of the aluminum-silicate-bearing rocks of the area are presented. However, petrographic data on all available samples (7) of the equigranular rocks are given because of significant differences among the samples.

SILLIMANITE GNEISS

Quartz, orthoclase, and plagioclase (oligoclase to andesine) are the most abundant felsic constituents of the gneiss, and together generally compose one-quarter to one-half of the rock (table 2). Quartz most commonly occurs as small, flattened lenticles 1 or 2 mm in length, aligned along the foliation. Grains characteristically have undulose extinction and sutured margins, indicating that there was little recrystallization after deformation. Orthoclase (identified by X-

ray diffraction) is present as small (1 to 2 mm in diameter) untwinned xenoblastic grains. Perthitic intergrowths are very rare. Plagioclase is similar in size to quartz and orthoclase, but it is generally subidioblastic. In some samples of gneiss, plagioclase is elongate and xenoblastic, showing iron staining along abundant fractures. Polysynthetic twins are common and are offset by the fractures in some thin sections. Concentric zoning is indicated in a few grains by differential extinction. Sericitization of feldspar grains generally is minor.

Biotite is the dominant mica, making up half or more of the rock and giving the overall dark aspect to the gneiss. In thin section, the grains show red-brown to tan pleochroism. They are lens-shaped or subidioblastic or idioblastic, depending on the relative amounts of recrystallization following cataclasis. Subequant biotite grains with ragged margins are common. Biotite is slightly altered locally to a mixture of chlorite and rutile or, rarely, sericite. More extensive alteration has been observed in only a few thin sections, where "islands" of biotite occur in a "sea" of sericite.

In some of the more schistose samples, particularly those near the northern gneiss-schist contact (fig. 2), muscovite is interleaved with biotite. Where muscovite is present, it generally makes up only a few percent of the rock (table 1) and consists of small, ragged grains.

Sillimanite occurs as fibrolite mats, as small colorless needles, and as well-formed prisms (fig. 5A). All three forms are commonly observed in the same thin section. Some bundles of fibrous sillimanite reach up to ½ cm in length and develop cross fractures similar to the transverse partings of a single prism (fig. 5B). The average length of the sillimanite fibers or grains is 1 to 2 mm, but grains 5 mm long are common in the center of the gneiss body. Thin, wavy streams of fibrolitic sillimanite commonly define the foliation. In many thin sections, sillimanite is intergrown with biotite, giving the impression that it is replacing biotite. All ranges of the degree of intergrowth of the two minerals, from minor amounts of sillimanite needles at the edges of biotite grains to abundant needles and mats of sillimanite within biotite, can be observed in thin section (fig. 5C). In the most advanced stages of what appears to be replacement by sillimanite, biotite remains as indistinct remnants, commonly with pale, "bleached," tan pleochroism. Although sillimanite is associated most commonly with biotite, in some samples it is concentrated between quartz or feldspar grain boundaries. Rarely, it is found as inclusions within quartz, orthoclase, and cordierite.

25	76AFr236	-----do.-----	Lepidoblastic	M M tr m m tr - - - tr - tr	X X - - X	- - X
26	77AFr4090	-----do.-----	Homeoblastic, crudely lepidoblastic	m m tr M M tr - - - - -	X - X	- -
28	77AFr41028	-----do.-----	Lepidoblastic	tr M tr tr M m - - - - -	X X - -	- -
28	77AFr41103	-----do.-----	Lepidoblastic, intensely deformed	tr M - tr m M - - - - M	X - - X	- -
29	72AMr498	-----do.-----	Lepidoblastic	m m tr tr M m - - - - M	X X - -	- X
30	77AMr1500	-----do.-----	Lepidoblastic, homeoblastic	m M tr m M tr - - - tr - -	X X - -	- -
31	72AMr46	Granitic-appearing rock	Equigranular with slight alignment of micas	M tr tr m M tr - - - - -	X X X	- -
32	77AMr163	Gneiss	Cataclastic, lepidoblastic	M M m tr m tr - - - - -	X X - -	- -
33	64APw3	Granitic-appearing rock	Equigranular	m tr tr tr M tr - - - - -	X X - -	- -
34	77AFr4118	Gneiss	Lepidoblastic	m M - - M m - - - - -	X X - -	- -
35	77AFr4112	Granitic-appearing rock	Equigranular with slight preferred orientation	m tr tr M M tr tr - - - - -	- X - -	- -
36	77AFr4111	Gneiss	Lepidoblastic	m M - tr M m - - - - -	X - - -	- -
37	77AMr185A	-----do.-----	-----do.-----	M M tr tr tr m - - - - tr	X X - -	- -
38	77AMr194B	-----do.-----	-----do.-----	m M - m M tr - - - - tr	X X - -	- -
39	77AFr4123B	Granitic-appearing rock	Equigranular	m tr tr m M tr - - - - -	- X - -	- X
40	77AFr4140	Gneiss	Lepidoblastic, cataclastic	M m tr M tr tr - - - - -	X X - -	- -
41	77AFr3020	Gneiss	-----do.-----	m M - tr M m - - - - -	X X - -	- -

Andalusite, rather than sillimanite, is the only Al_2SiO_5 polymorph in one sample of biotite gneiss from the southwestern part of the gneiss body (fig. 2). It occurs in a thin micaceous layer several millimeters wide as elongate xenoblasts 1 to 3 mm long, and it shows pink pleochroism in places. Nearby samples of gneiss contain sillimanite and no andalusite. Andalusite, together with sillimanite, is present in several rocks which have equigranular textures; those rocks are discussed in the next section.

Cordierite was identified optically in a total of eleven samples of sillimanite-biotite-orthoclase gneiss, most of which came from the central part of the gneiss body (fig. 2). Petrographic identification was confirmed by the electron microprobe. Typical cordierite-bearing assemblages are given in table 1. Cordierite occurs most commonly as elongate xenoblastic grains several millimeters in length which include trains of minute sillimanite needles and small biotite flakes (fig. 5D), but more equant, smaller grains of cordierite are not unusual. Incipient alteration of cordierite to pinite is present to varying degrees in some thin sections, but overall, the cordierite is relatively fresh. Local alteration of cordierite to a serpentine-group mineral was observed in several grains in two thin sections.

Garnet, zircon, tourmaline, apatite, and rutile, in decreasing order of abundance, occur as accessory minerals (table 2). Garnets are generally small idiomorphs or granules less than 0.5 mm in diameter around which there is little deflection of biotite folia. Zircons are smaller than the other accessory minerals and are most common as small inclusions with pleochroic halos in biotite. Tourmaline is present only locally as small (1 mm long) subidioblasts with bluish-green to yellow pleochroism, which only rarely are zoned. Minute, nearly opaque blebs and needles or, rarely, yellowish to reddish-brown granules of rutile occur in chlorite which has replaced biotite. The only opaque mineral positively identified by means of the microprobe is ilmenite.

EQUIGRANULAR FELDSPATHIC ROCKS

In seven different localities within the gneiss body or, in the case of one sample, in schist just north of the body, rocks that have equigranular, igneous-appearing textures are found to contain sillimanite, sillimanite+andalusite, or sillimanite+andalusite+garnet in thin section. Textural features indicative of both igneous and metamorphic processes are present in these rocks. The locations of these samples are shown on figure 2 (localities 14, 15, 17, 31, 33, 35, and 39) and their complete mineral assemblages in table

2. All of the samples contain more than 30 percent modal orthoclase, which is not an unusual amount for the areas in which these rocks are found; nearby sillimanite gneiss is also high in orthoclase (see table 2 and fig. 2). In most of the aluminum-silicate-bearing equigranular rocks, the development of sillimanite is similar to that in the foliated rocks, in which fibrolite is intergrown with biotite (localities 17, 31, 33, and 35), or, as in a few schist samples, has grown as a fringe around andalusite (fig. 5E) (localities 17, and 35) or as needles within it (locality 15) indicating that the rocks have been metamorphosed. A very subtle alinement of biotite and muscovite grains was observed in two samples (localities 14 and 15), and andalusite prisms as well are crudely alined in the sample from locality 35. Incipient cataclastic foliation, suggested by a planar fabric of sutured contacts and granulation between grains, also occurs in the equigranular rocks from localities 14 and 15.

However, there are important differences between the equigranular aluminum-silicate-bearing rocks and surrounding sillimanite gneiss. Unlike the sillimanite gneiss, many of the more equigranular rocks are characterized by: (1) a total or nearly total lack of preferred mineral orientation (localities 17, 31, 33, 39, and 14, 15, 35, respectively), (2) grains of andalusite, as well as sillimanite (localities 14, 15, 17, and 35), (3) halos of muscovite which rim several grains of andalusite (localities 14 and 15) and garnet (locality 14), (4) oscillatory zoning in plagioclase laths (fig. 5F) (localities 17, 31, and 33), (5) highly perthitic potassium feldspar (localities 14, 15, 17, 31, and 33), or (6) development of myrmekite along the margins of some plagioclase grains (localities 14, 15, 17, and 33).

At three localities, field relations suggest an intrusive relationship: samples from localities 14 and 15 were collected from rocks which cut the surrounding sillimanite gneiss, and the sample from locality 31 was taken from a knoll of granitic-appearing rock which crops out in the center of the gneiss body. Three other samples (localities 17, 35, and 39) were collected from areas of granitic-appearing rubble in which more gneissic rubble is also present. Information about the geologic setting of the sample from locality 33 is not available. The origin of these aluminum-silicate-bearing, equigranular rocks is discussed later in this paper.

PELITIC SCHIST

Biotite and muscovite in well-formed books are the major constituents of the schistose rocks. Sheaves of both micas, 1 to 3 mm long, typically are interleaved and form continuous folia several millimeters

wide. In a small number of thin sections, a minor amount of biotite or muscovite lies at an angle to the foliation. Chloritization of biotite or sericitization of muscovite is minor. Chlorite occurs as discrete crystals in a small number of samples; it is more common in the northern part of the area mapped as schist (see table 2 and fig. 2).

Alternating with the mica folia are bands composed of quartz, plagioclase (oligoclase or andesine), and potassium feldspar. These minerals are more coarsely grained in the schist than in the gneiss, with crystals commonly up to 5 mm in length. Quartz is strained and shows sutured grain boundaries between polycrystalline segments of elongate bands and lenses. Subhedral plagioclase laths display well-formed polysynthetic twins, some of which have deformed lamellae. Potassium feldspar is rare in the schists and where present consists of untwinned small xenoblasts. Feldspar is generally fresh and has only minor sericitization or kaolinitization.

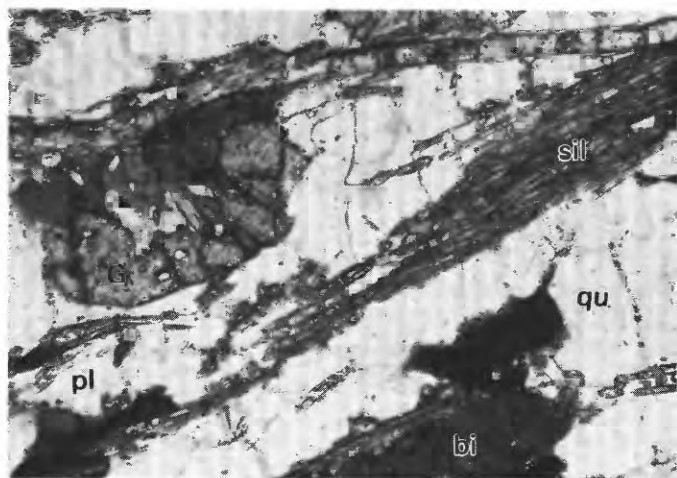
Subidioblastic or idioblastic garnet porphyroblasts averaging 1 or 2 mm but reaching as much as 1 cm in diameter are common in the pelitic schist. A few of the large garnets have rotational and snowball structures, evidenced by a spiral pattern of ilmenite and (or) quartz inclusions, which indicate syntectonic crystallization (Spry, 1969, p. 253). Most, but not all, of the garnet porphyroblasts deflect mica folia. A

small percentage of garnets have a weblike appearance caused by the large number of quartz inclusions which have grown to cut off segments of the crystal. Alteration of garnet to chlorite is minor. In a few thin sections, small lens-shaped knots composed of biotite, muscovite, quartz, and fibrolite replace garnet (fig. 5G). Small granules of relict garnet are present in some of these knots. Fresh euhedral garnets, partially replaced garnets, and wholly replaced garnets may occur together in a single thin section.

Strongly colored yellow pleochroic porphyroblasts of staurolite are seen in most thin sections of pelitic schist. The crystals are typically stubby subidioblastic prisms or small granules, 1 to 2 mm in length, some of which poikilitically enclose minute quartz grains. Staurolite is commonly concentrated in layers, associated with and next to garnet or kyanite porphyroblasts, with which it is in apparent textural equilibrium (fig. 5H). Staurolite does not generally deflect the foliation. In one sample, a band of staurolite crystals is bowed around a large garnet porphyroblast. These textural relations may indicate either that the crystallization of garnet predates that of staurolite or that garnet formed later than staurolite and pushed out the preexisting foliation that contained the staurolite porphyroblasts (see Misch, 1971, for a discussion of the "crystallization force" of porphyroblasts).

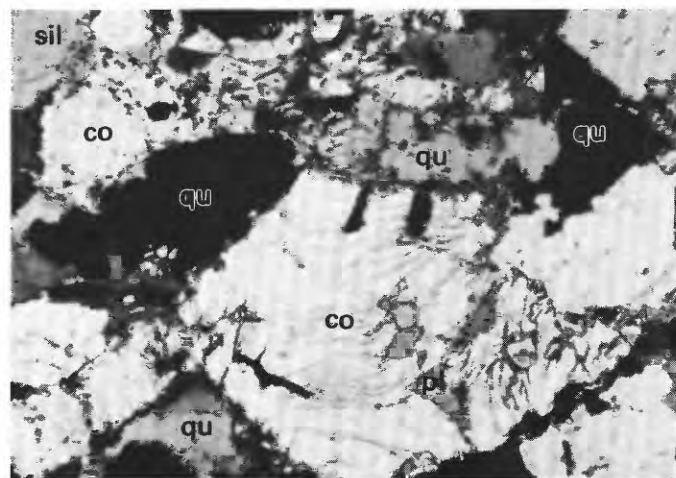
FIGURE 5 ON PAGES 12-13

FIGURE 5.—Photomicrographs showing textural relations in sillimanite gneiss, equigranular feldspathic rock, and pelitic schist. Andalusite (A); biotite (bi); cordierite (co); fibrolite (F); garnet (G); kyanite (ky); muscovite (mu); orthoclase (or); plagioclase (pl); quartz (qu); sillimanite (sil); staurolite (st). **A**, Prismatic sillimanite in garnetiferous sillimanite gneiss from north-central part of gneiss body (locality 22, fig. 2). Sillimanite occurs adjacent to garnet, in quartz folia, and within and around biotite. Note transverse partings in largest sillimanite prisms. Plane-polarized light. **B**, Sheaflike mats of fibrolite with transverse partings (locality 27, fig. 2) in sillimanite gneiss. In this sample (from central area of gneiss body), fibrolitic sillimanite occurs adjacent to quartz grains rather than biotite, as more commonly is the case. Plane-polarized light. **C**, Finely acicular sillimanite that appears to be replacing biotite in cordierite-sillimanite gneiss from central part of gneiss body (locality 28, fig. 2). Plane-polarized light. **D**, Xenoblastic cordierite from central part of gneiss body (locality 29, fig. 2). Note dark alteration (chlorite?) along cracks and preferential concentration of minute grains of sillimanite and biotite within cordierite. Crossed polarizers. **E**, Zoned andalusite grain rimmed by fringe of fibrolitic sillimanite in equigranular feldspathic rock (locality 17, fig. 2). Plane-polarized light. **F**, Oscillatory zoning in plagioclase grain in same rock as *E*. Crossed polarizers. **G**, Nearly total replacement of garnet porphyroblast in staurolite-3-aluminum silicate-quartz-mica schist north of the Salcha River (locality 4, fig. 2). Deflection of foliation around knot of remnant garnet granules, biotite, quartz, minor muscovite, and fibrolite outlines area of former porphyroblast. Crossed polarizers. **H**, Association of staurolite, kyanite, and garnet in 3-aluminum-silicate-bearing schist east of the gneiss body (locality 9, fig. 2). Staurolite shares common grain boundary with kyanite, evidence of their equilibrium relationship. Plane-polarized light. **I**, Acicular fringe of sillimanite that has grown on margin of small andalusite xenoblast in staurolite-bearing quartz-mica schist east of South Fork of the Salcha River (locality 10, fig. 2). Andalusite and sillimanite present in trace amounts only. Opaque mineral is probably ilmenite. Plane-polarized light. **J**, Kyanite included in and growing on margin of andalusite porphyroblasts in garnetiferous staurolite-kyanite-andalusite-biotite schist east of South Fork of the Salcha River (locality 11, fig. 2). Textural relations imply that kyanite crystallized before andalusite. Plane-polarized light. **K**, Irregularly shaped patch of staurolite adjacent to fibrolitic sillimanite in sample of garnet-staurolite-3-aluminum silicate-mica schist, north of the Salcha River near its North Fork (locality 8, fig. 2). Appearance of staurolite in photo and its spongy appearance due to numerous quartz inclusions elsewhere in thin section suggest staurolite may be unstable. Fibrolitic sillimanite is associated with biotite, from which at least part of it may have formed. The proximity of unstable staurolite and apparently newly crystallized sillimanite also allow the possibility that staurolite may have been consumed in a sillimanite-producing reaction. Plane-polarized light. **L**, Fibrolitic sillimanite and andalusite growing on opposite ends of the same biotite crystal in sample of figure 5G. Note continuation of biotite in matrix into andalusite xenoblast. Fibrolitic sillimanite is present in trace amounts and appears to replace biotite. Plane-polarized light.



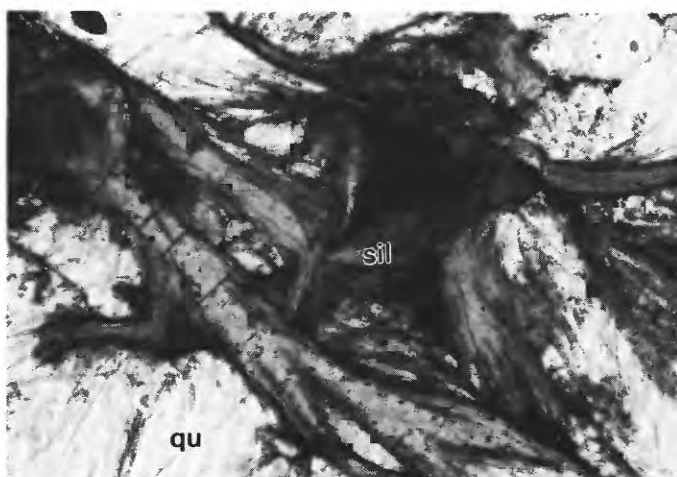
A

0 0.5 mm



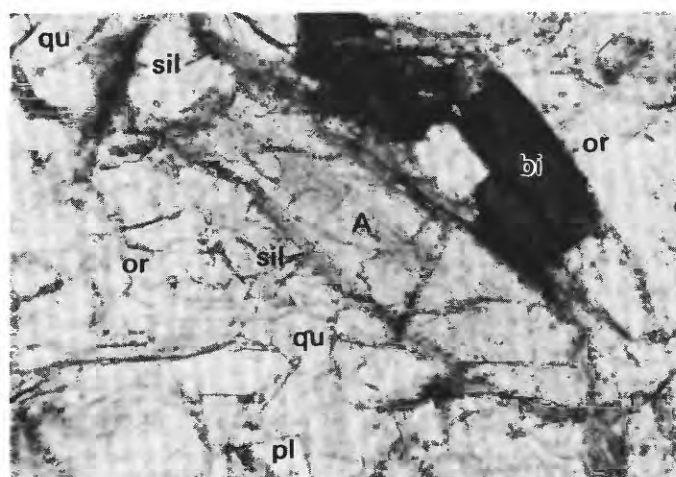
D

0 1.0 mm



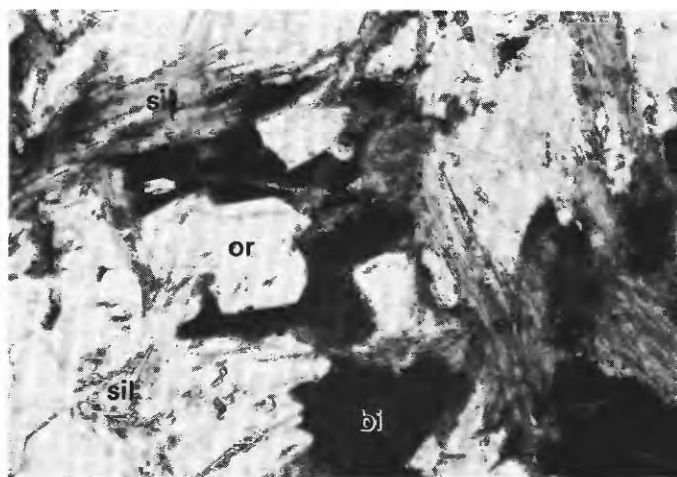
B

0 0.5 mm



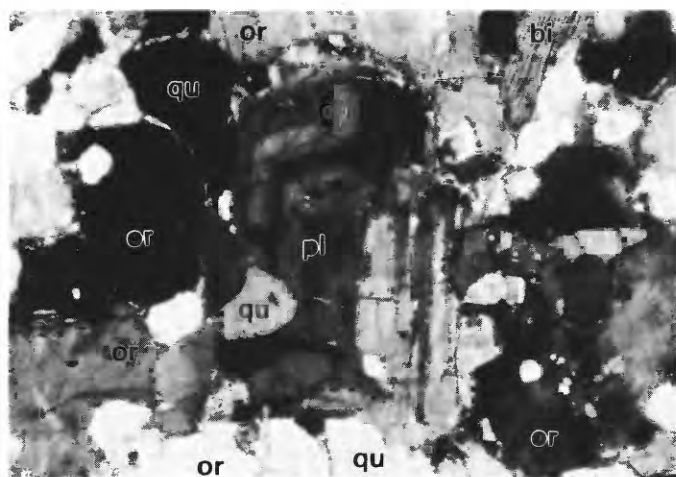
E

0 0.5 mm



C

0 0.5 mm



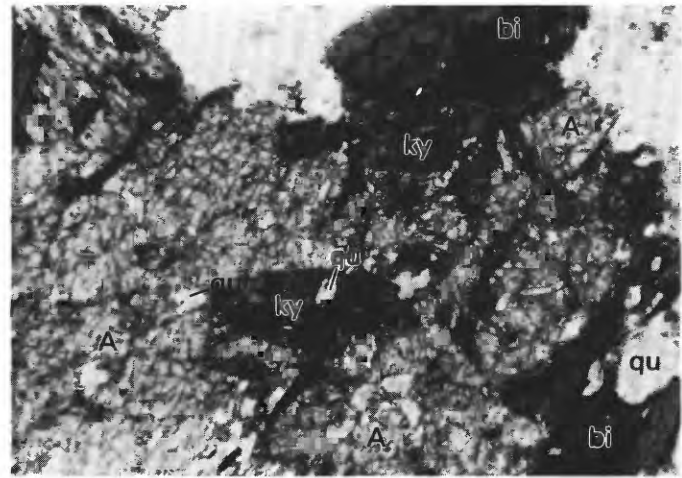
F

0 1.0 mm

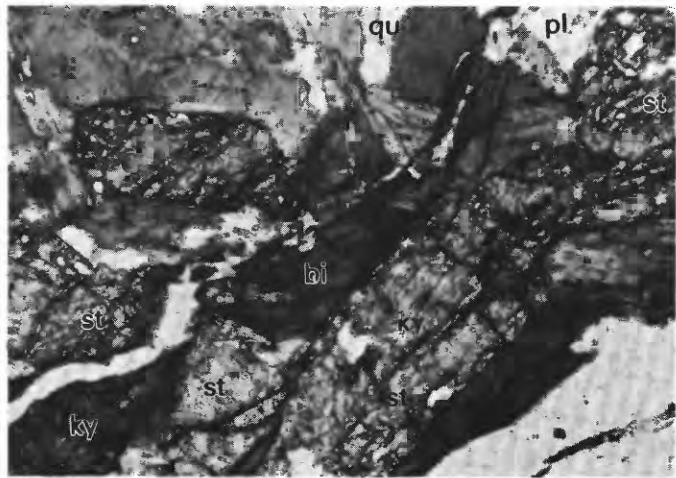
FIGURE 5.—Continued.



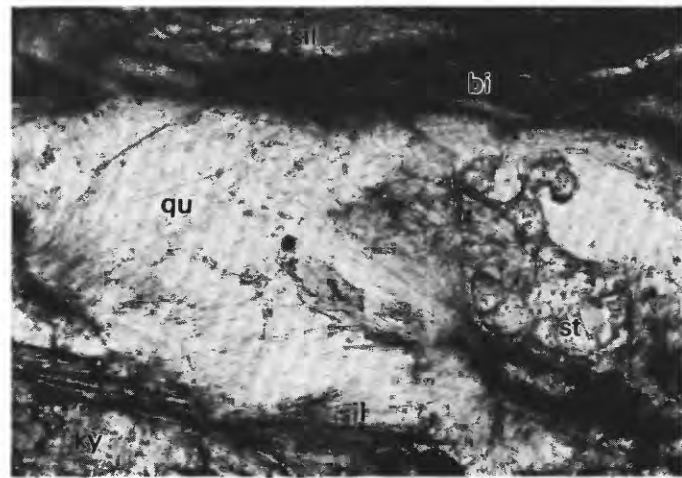
G



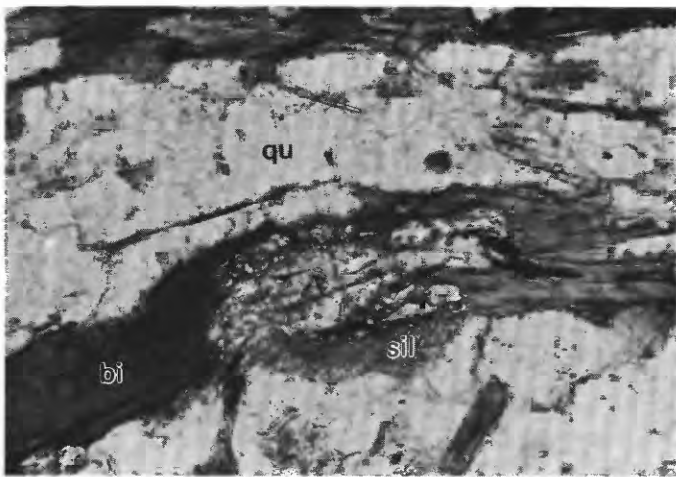
J



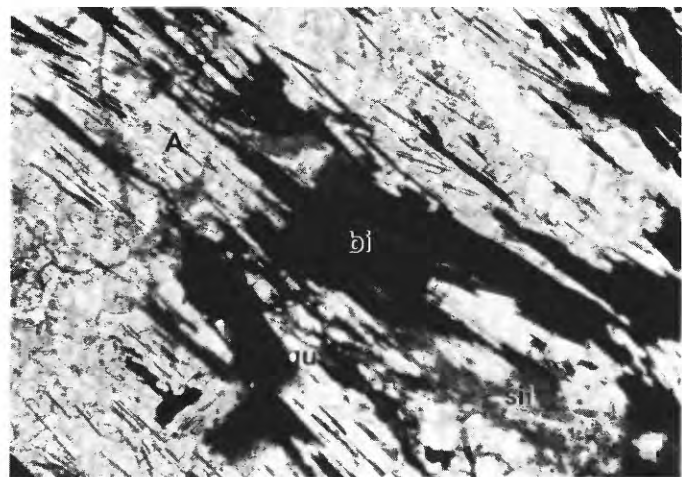
H



K



I



L

FIGURE 5.—Continued.

Andalusite is generally the largest and most abundant aluminum silicate polymorph in the quartz-mica schists; it occurs as colorless or faintly pink elongate xenoblasts, 1 or 2 cm long, enclosing abundant needlelike biotite flakes that are parallel to foliation. Inclusions of staurolite are present in a few andalusite grains. In several thin sections, andalusite forms a small mass in the middle of muscovite folia, with an irregular contact between the two minerals. Andalusite is rarely in direct contact with any of its polymorphs, but in the three staurolite-sillimanite-andalusite-bearing schist samples which are found within ½ km of one another just east of the South Fork of the Salcha River (fig. 2), a narrow fringe of acicular sillimanite has grown around part of an andalusite porphyroblast (fig. 5I), and in another locality just a few kilometers away, kyanite occurs within and adjacent to an andalusite porphyroblast (fig. 5J).

Kyanite is the next most abundant aluminum silicate; it occurs as small, stubby idiomorphs or subidiomorphs, less than 2 mm long, which are generally surrounded by or adjacent to biotite or muscovite. In one thin section, kyanite has grown in the middle of a large crystal of muscovite. Kyanite, which is typically elongate in a plane parallel or nearly parallel to the foliation, does not deflect micaceous foliation. Only in one thin section do kyanite prisms lie at an angle to the foliation, and even in this thin section, most of the prisms do not.

Fibrolitic sillimanite is present in small or trace amounts in most thin sections of pelitic schist. There is a general increase in the amount of sillimanite in the schist toward the schist-gneiss contact. As in the samples from the gneiss body, fibrolitic or finely acicular sillimanite has nucleated adjacent to and within biotite grains, generally parallel to foliation. In a few samples, minor amounts of sillimanite occur within some grains of quartz or feldspar. In one thin section (locality 8, fig. 2), needles of sillimanite occur next to a small, irregularly shaped bleb of staurolite (fig. 5K). These textural relations may indicate staurolite was consumed partially in a sillimanite-producing reaction.

Several different combinations of the Al_2SiO_5 polymorphs are commonly only millimeters apart in the samples. Andalusite, kyanite, and sillimanite occur together in single thin sections from four separate localities (see fig. 2), 6 to 15 km apart in a linear zone. The modes of occurrence of the aluminum silicates and the textures and mineralogy in these samples are identical to those described above. Although no aluminum silicate polymorphs in any of the four thin sections directly touch one another, in one thin section (fig. 5L) both sillimanite and andalusite are

present on opposite sides of a biotite grain, and in another sample sillimanite and kyanite are also seen on opposite sides of a biotite grain. These associations suggest that these pairs of aluminum silicates are both stable with biotite and probably are also stable with one another.

Tourmaline prisms averaging 2 mm in length, commonly with zonal structure, are present in many pelitic schist samples. Pleochroic colors of gray, bluish gray, and olive suggest that the mineral is the iron-rich tourmaline, schorlite. Other accessory minerals, in order of decreasing abundance, are zircon, apatite, rutile, ilmenite, hematite, and sphene. Small amounts of magnetite and graphite may also be present, but all the opaques identified thus far by microprobe have been ilmenite.

GEOTHERMOMETRY BASED ON COEXISTING GARNET AND BIOTITE IN PELITIC SCHIST AND SILLIMANITE GNEISS

The distribution of Fe and Mg between garnet and biotite provides a way to determine, independent of the implications of the distribution of aluminum silicate minerals, the temperatures at which the minerals equilibrated in the pelitic schist and sillimanite gneiss. Similar geothermometry has been applied successfully to many other pelitic rocks (e.g., Ghent and others, 1979; Baltatzis, 1979; and Labotka, 1980, to list a few of the recent papers). We viewed the geothermometric results in terms of three problems: (1) Is there a systematic increase in temperature toward the center of the gneiss body which would support the hypothesis that it is a gneiss dome? (2) Was the temperature in the sillimanite gneiss body high enough to produce in situ formation of granitic melt? (3) Are equilibrium temperatures indicated for the schist samples that contain all three aluminum silicates?

Garnet-biotite pairs were analyzed by electron microprobe in 11 samples of aluminum-silicate-bearing rocks from 9 different localities. Complete analyses were made of 29 garnet-biotite pairs; only two of the four samples containing all Al_2SiO_5 polymorphs had garnet-biotite pairs with apparent equilibrium textures. Each value represents an average of at least six closely spaced points. In all cases but one, biotite and garnet were in physical contact with one another and were analyzed very near their mutual contact.

Representative microprobe analyses of biotite are presented in table 3 and of garnet in table 4. Temperatures based on the calibrations of Goldman and Albee (1977), Thompson (1976), and Ferry and Spear (1978)

TABLE 3.—Representative chemical analyses of biotite

[Analyses by electron microprobe, using natural and synthetic mineral standards and the Z.A.F. matrix correction program FRAME (Yakowitz and others, 1973). C. R. Bacon, analyst]

Sample number (see fig. 16 for location)	75AWr 784A	77AFr 46E	76AFr 197B	76AFr 272C	75AFr 981	76AFr 241	77AWr 150D	76AFr 4115A
Crystal rim	1A	1	2	^a 2	1	1	2	1
SiO ₂ -----	35.7	35.4	36.7	34.9	35.2	35.3	34.9	35.0
Al ₂ O ₃ -----	20.4	20.3	19.8	21.3	21.3	20.8	20.8	20.1
FeO ^b -----	21.3	20.0	20.4	21.8	20.0	20.5	19.2	21.1
MgO-----	8.29	8.29	8.94	7.72	9.05	7.42	7.99	7.76
CaO-----	.04	.07	.02	.04	.02	.03	.03	.01
Na ₂ O-----	.16	.17	.21	.16	.31	.19	.17	.15
K ₂ O-----	9.18	8.69	8.72	8.73	8.98	9.45	9.16	9.74
TiO ₂ -----	1.73	1.17	1.31	1.40	.90	2.88	2.41	2.97
MnO-----	.13	.04	.15	.14	.08	.31	.28	.27
Cl-----	.01	.02	.02	.02	.00	.01	.00	.00
F-----	.27	.32	.26	.22	.32	.17	.25	.22
H ₂ O ^c -----	3.85	3.74	3.86	3.84	3.82	3.90	3.82	3.87
Less O-----	.12	.14	.11	.10	.13	.07	.11	.09
Total-----	100.94	98.07	100.28	100.17	99.85	100.89	98.90	101.10

Mineral formulae on the basis of 24 anions

Si-----	5.350	5.415	5.491	5.277	5.297	5.295	5.302	5.269
Al-----	3.603	3.660	3.491	3.796	3.777	3.677	3.724	3.566
Fe-----	2.670	2.559	2.552	2.757	2.517	2.572	2.440	2.657
Mg-----	1.852	1.891	1.994	1.740	2.030	1.659	1.810	1.742
Ca-----	.006	.011	.003	.006	.003	.005	.005	.002
Na-----	.046	.050	.061	.047	.090	.055	.050	.044
K-----	1.755	1.696	1.664	1.684	1.724	1.808	1.775	1.871
Ti-----	.195	.135	.147	.159	.102	.325	.275	.336
Mn-----	.017	.005	.019	.018	.010	.039	.036	.034
Cl-----	.003	.005	.005	.005	.000	.003	.000	.000
F-----	.128	.155	.123	.105	.152	.081	.120	.105
Temperature °C ^d ---	549	541	540	601	592	655	678	721

^aBiotite inclusion in garnet 2.

^bTotal Fe as FeO.

^cH₂O calculated assuming full hydroxyl site occupancy and no ferric iron, with OH equal to 2-F-Cl.

^dEquilibration temperature for coexisting biotite and garnet calculated from Ferry and Spear (1978).

are presented in table 5. The highest temperature garnets tend to have relatively low Ca and high Mn values, and the Ti in biotite seems to increase with temperature. All of the samples fall within or close to the compositional limits of the calibration of the geothermometer given by Ferry and Spear (1978).

Cores and rims of three garnet porphyroblasts were analyzed. In the two garnets for which the highest temperatures were calculated (77AWr150D and 76AFr4115A, table 4), there was a decrease between cores and rims in Fe, Mg, and Ca and an increase in

Mn, whereas for the lower temperature sample (77AFr46E), all the trends were reversed except for that of Ca. Insufficient data preclude generalization about the zoning trends which may be present in the garnets. Inclusions in garnet, identified by microprobe, are (in decreasing order of abundance): quartz, ilmenite, rutile, and rare pyrite.

Estimated temperatures (table 5) for garnet-biotite pairs (in direct contact and in apparent textural equilibrium) within a single one-inch-diameter polished thin section agreed to better than 20°C in almost

TABLE 4.—Representative chemical analyses of garnet

[Analyses by electron microprobe, using natural and synthetic mineral standards and the Z.A.F. matrix correction program FRAME (Yakowitz and others, 1973). C. R. Bacon, analyst]

Sample number (see fig. 16 for location)	75AWr 784A	77AFr 46E	77AFr 46E	76AFr 197B	76AFr 272C	75AFr 981	76AFr 241	77AWr 150D	77AWr 150D	76AFr 4115A	76AFr 4115A
Crystal	1 rim	1 core	1 rim	2 rim	^a 2	1 rim	1 rim	2 core	2 rim	1 core	1 rim
SiO ₂ -----	37.8	37.3	37.6	37.3	37.5	37.6	37.1	37.8	37.3	37.5	37.6
Al ₂ O ₃ -----	21.3	21.2	21.4	21.1	21.3	21.2	20.8	21.8	21.4	21.4	21.2
FeO ^b -----	34.7	34.5	35.4	31.7	33.6	34.9	31.4	32.0	30.8	31.5	31.1
MgO-----	2.22	1.20	2.35	2.22	2.28	2.95	2.51	4.04	2.99	3.10	2.94
CaO-----	4.62	6.72	3.99	2.73	4.17	3.39	1.27	1.86	1.31	1.42	1.54
Na ₂ O-----	.02	.02	.02	.01	.02	.01	.01	.01	.01	.01	.02
TiO ₂ -----	.09	.09	.10	.02	.06	.05	.05	.05	.03	.02	.04
MnO-----	.62	.75	.33	5.69	2.58	.30	7.69	3.23	6.42	5.78	6.66
Total-----	101.37	101.78	101.19	100.77	101.51	100.40	100.83	100.79	100.26	100.73	101.10
Mineral formulae on the basis of 24 oxygens											
Si-----	5.999	5.940	5.982	5.988	5.964	6.007	5.979	5.979	5.986	5.990	5.998
Al-----	3.984	3.979	4.012	3.992	3.992	3.991	3.950	4.064	4.048	4.029	3.986
Fe-----	4.606	4.595	4.710	4.256	4.469	4.663	4.232	4.233	4.134	4.208	4.149
Mg-----	.525	.285	.557	.531	.540	.703	.603	.953	.715	.738	.699
Ca-----	.786	1.147	.680	.470	.711	.580	.219	.315	.225	.243	.263
Na-----	.006	.006	.006	.003	.006	.003	.003	.003	.003	.003	.006
Ti-----	.011	.011	.012	.002	.007	.006	.006	.006	.004	.002	.005
Mn-----	.083	.101	.044	.774	.348	.041	1.050	.433	.873	.782	.900
Temperature °C--	549		541	540	601	592	655		678		721

^aGarnet analyzed adjacent to biotite inclusion.

^bTotal Fe as FeO.

^cEquilibration temperature for coexisting biotite and garnet calculated from Ferry and Spear (1978).

all determinations and to within 10°C in over half of the determinations. No reliable temperature estimates were obtained for the two samples (76A Fr272A and 77A Wr387C) that contain all three aluminum silicate polymorphs, because the garnet-biotite pairs analyzed were not totally fresh and appeared not to be in equilibrium with each other and the surrounding phases. The textural and mineralogical similarity between these two andalusite-kyanite-sillimanite-bearing samples and the five other samples of pelitic schist (three of which contain more than one Al_2SiO_5 polymorph) for which temperature data were consistent (table 5) suggests that equilibrium conditions in which andalusite, kyanite, and sillimanite are stable together may indeed have existed locally.

Agreement between garnet-biotite temperatures calculated from Thompson's and Ferry and Spear's calibration is generally good, agreeing to within 15°C for over half the determinations and to within 30°C for all but a few determinations. Agreement is not as good, however, between the former two calibrations and that of Goldman and Albee; most temperatures calculated to the latter's calibration are lower by about 30°C to 80°C. In general, there is better agreement between Goldman and Albee's calibration and the other two calibrations (table 5) in pelitic schist than there is in the higher temperature sillimanite gneiss. Ghent and others (1979) reported similar good agreement between temperatures calculated from the calibrations of Thompson (1976) and Ferry and Spear (1978) and poor agreement between those two calibrations and that of Goldman and Albee (1977). Goldman and Albee (1977) suggest that the source of a possible problem with their calibration might be inaccuracies in the experimental calibration of oxygen-isotope fractionation (with which their calibration is correlated) at higher temperatures. Ghent and others (1979) argue that the poor agreement could also be due to cessation of $^{18}\text{O}/^{16}\text{O}$ exchange at lower temperatures than those permitting Fe/Mg exchange.

The temperatures reported here for garnet-biotite equilibration are based on an assumed pressure of 0.4 GPa, but because exchange equilibria are virtually independent of variation in pressure, the temperatures change by only about 5° per GPa for these samples. Estimates of the analytical precision of our data, based entirely on microprobe analytical error, suggest that an uncertainty of $\pm 30^\circ$ is very conservative for relative temperatures in this study. Absolute temperatures, however, may be subject to greater uncertainty. The rounded averages of temperature data for garnet-biotite pairs considered to be in equilibrium are given for the three calibrations in separate columns in table 5 headed "Averaged

G-A, T, and F-S." In order to simplify discussion, and because the averaged temperature data for the Ferry and Spear and the Thompson calibrations differ very little in their absolute values, the averaged temperatures calculated from Ferry and Spear's calibration are referred to in the text and their areal distribution is shown in figure 6.

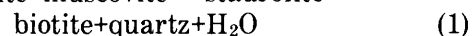
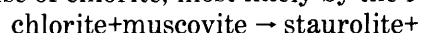
The highest temperature ($705^\circ \pm 30^\circ\text{C}$) was determined for a sample of typical, fine-grained, "salt and pepper" sillimanite gneiss from the center of the body (76A Fr4115A, fig. 6, tables 2-4). Samples of similar gneiss to the west and south yielded slightly lower temperatures of 655° and $670^\circ \pm 30^\circ\text{C}$. Equilibration temperatures reported for samples of garnet-staurolite-aluminum-silicate-bearing schist (535° to $600^\circ \pm 30^\circ\text{C}$) are appreciably lower than the values determined for samples of sillimanite gneiss.

DISCUSSION

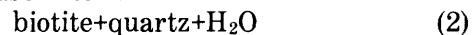
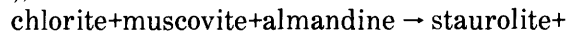
METAMORPHIC REACTIONS AND ISOGRADS IN PELITIC SCHIST AND SILLIMANITE GNEISS

STAUROLITE+BIOTITE ISOGRAD

The northernmost isograd shown in figure 2 marks the first appearance of staurolite with biotite. North of the staurolite+biotite isograd, rocks are lower in grade (epidote-amphibolite facies, Thompson and Norton, 1968), consisting of muscovite+chlorite+quartz \pm biotite \pm plagioclase \pm garnet assemblages. Because chlorite is common north (downgrade) of this isograd and is rare south of it (see table 1), the staurolite-producing reaction which defines this isograd is believed to be one in which staurolite forms at the expense of chlorite, most likely by the reactions:

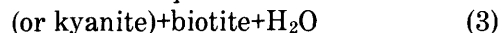
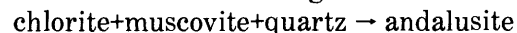


(modified from equation 26, Thompson and Norton, 1968), or



(equation 22, Thompson and Norton, 1968).

The first appearance of staurolite with biotite coincides with the first appearances of kyanite, andalusite, and sillimanite. Pelitic schist that occurs up-grade of this isograd will be referred to as being in the staurolite-aluminum silicate zone. Within this zone, andalusite appears to have developed at the expense of muscovite according to the reaction:



(modified from equation 16, Thompson and Norton, 1968). The presence of needlelike grains of biotite

TABLE 5.—Distribution coefficients for the Fe/Mg ratio in coexisting garnet and biotite and equilibration temperatures (in degrees Celsius) calculated at 0.4-GPa total pressure

[K_D calculated from microprobe analyses of garnet and biotite adjacent to mutual contacts. Temperatures calculated from Goldman and Albee (1977) (G-A), Thompson (1976) (T), and Ferry and Spear (1978) (F-S). Averaged (Avg) temperatures are rounded averages of temperature data for garnet-biotite pairs considered to be in equilibrium. Uncertainty in temperatures due to analytical error estimated to be ±30°C. Key minerals, listed in decreasing order of abundance: mu, muscovite; st, staurolite; a, andalusite; ky, kyanite; sil, sillimanite; trace amounts indicated by parentheses. All samples contain quartz and feldspar]

Sample number (see fig. 16 for location)	Key minerals	Rock type	Crystal number		Garnet				Temperature (°C)							
			Garnet	Biotite	X _{Mn}	X _{Ca}	X _{Fe}	X _{Ti}	X _{AlVI}	K _D	G-A	Avg G-A	T	Avg T	F-S	Avg F-S
77AWr387C	mu, st, ky,	Schist	1	1	0.006	0.157	0.530	0.023	0.203	0.273	±771	---	±718	---	±749	---
	a, sil		3	3	.013	.208	.522	.020	.212	.102	±479	---	±464	---	±422	---
75AWr784A	mu, st	-do.-	1	b ₁	.014	.131	.587	.029	.194	.240	±642	---	±675	---	±689	---
			1	1A	.014	.131	.590	.033	.193	.164	520	525	568	560	549	540
			2	2	.023	.141	.571	.036	.191	.177	±554	---	±586	---	±573	---
77AFr46A			3	3	.105	.121	.575	.035	.195	.151	527	---	548	---	522	---
	mu, a, st	-do.-	1	1	.013	.062	.597	.030	.228	.244	±607	---	±681	---	±697	---
			2	2	.083	.082	.583	.025	.212	.193	±572	---	±611	---	±603	---
77AFr46E			2	2A	.038	.056	.545	.013	.207	.184	±543	---	±598	---	±587	---
	mu, a ky	-do.-	1	1	.007	.114	.575	.023	.216	.160	519	520	562	560	541	535
76AFr197B	st		2	2	.035	.110	.557	.020	.191	.155	514	---	554	---	530	---
	mu, st (sil)	-do.-	1	1	.125	.078	.559	.017	.218	.158	541	540	559	570	537	545
76AFr272A			1A	1A	.121	.072	.560	.041	.190	.169	±536	---	±583	---	±558	---
	mu, a, st,	-do.-	2	2	.128	.078	.561	.025	.197	.160	534	---	562	---	540	---
76AFr272C	sil, ky		1	1	.033	.076	.645	.031	.185	.326	±689	---	±784	---	±846	---
	m, a, sil	-do.-	2	2	.074	.075	.637	.040	.193	.203	±545	---	±625	---	±621	---
			1	1	.064	.092	.603	.029	.206	.304	±736	---	±757	---	±806	---
			2	±2	.057	.117	.613	.027	.207	.192	568	570	609	610	601	600
			2	2A	.029	.127	.618	.025	.193	.249	±644	---	±687	---	±707	---

75AFr981	mu, a, st, ky	-do.-	1	.007	.097	.554	.017	.208	.187	.557	560	602	605	592	600
76AFr241	sil (mu)	Gneiss	1	.172	.036	.607	.056	.210	.221	.598	610	650	650	655	655
77AWr150D	sil (mu)	-do.-	1	.152	.043	.574	.048	.216	.223	.619	625	660	660	659	670
76AFr4115A	mu, sil	-do.-	1	.150	.044	.604	.058	.182	.257	.5633	620	677	690	692	705

^aNot considered to reflect equilibrium conditions of maximum metamorphism on the basis of petrographic criteria.

^bInclusion in garnet.

^cBiotite and garnet not in direct contact.

within andalusite xenoblasts (fig. 5L) may be due to the fact that both these phases are products of reaction 3. Alternatively, these biotite grains, which are parallel to and continuous with adjacent folia of biotite and muscovite, may be unreacted remnants of biotite that was formerly interleaved with the muscovite that reacted to form andalusite.

Textural evidence for the paragenesis of kyanite in the staurolite-aluminum silicate zone consists only of the one thin section in which kyanite is surrounded by muscovite and which suggests that the kyanite may have formed from muscovite, possibly also by reaction 3. Staurolite appears to be stable with kyanite and no textural evidence of its involvement in a kyanite-producing reaction was observed.

Rare textural evidence for the development of fibrous sillimanite in pelitic schist (fig. 2) within this same zone suggests two possible sillimanite-producing reactions that may have occurred locally. The tiny needles of sillimanite that form a fringe around small andalusite porphyroblasts, mentioned earlier and shown in figure 5I, may indicate that some sillimanite formed by a polymorphic transition from andalusite. Textural evidence for the development of sillimanite at the expense of staurolite (see fig. 5K) in a garnet-staurolite-andalusite-kyanite-sillimanite-bearing

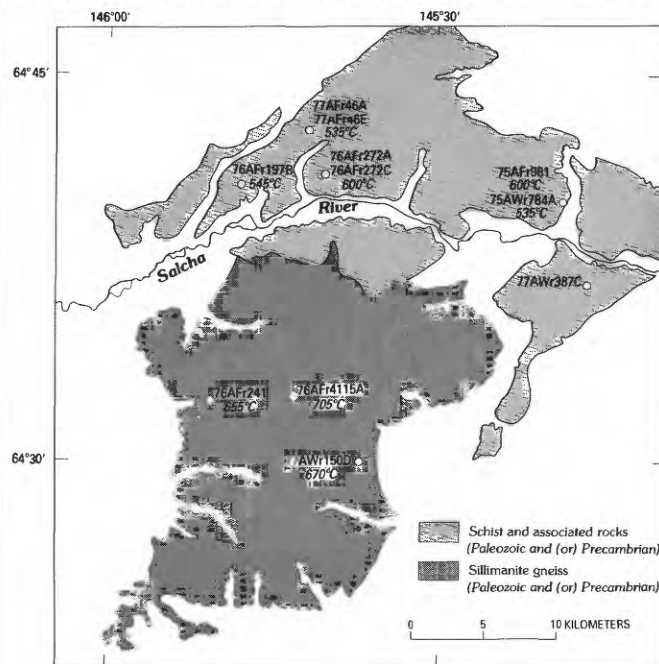


FIGURE 6.—Simplified geologic map of pelitic schist and sillimanite gneiss showing location of samples for which garnet-biotite pairs were analyzed and rounded averages of equilibrium temperatures calculated from Ferry and Spear (1978) (table 5).

schist (locality 8, fig. 2) suggests the reaction

$$\text{staurolite} + \text{muscovite} + \text{quartz} \rightarrow \text{sillimanite} + \text{almandine} + \text{biotite} + \text{H}_2\text{O} \quad (4)$$
 (equation 29, Thompson and Norton, 1968) may have occurred locally in the staurolite-aluminum silicate zone. However, because garnet+biotite+staurolite, garnet+biotite+staurolite+sillimanite, and staurolite+biotite+sillimanite all coexist with quartz and muscovite (and, in some samples, either andalusite or kyanite or both, shown in fig. 2), it is unlikely that this reaction can be used to explain all the occurrences of sillimanite in the pelitic schist. The development of sillimanite within the staurolite-aluminum silicate zone is not clearly the result of any one reaction.

With the exception of the one area east of the South Fork of the Salcha River where a fringe of sillimanite on andalusite may indicate a polymorphic transition, all three Al_2SiO_5 modifications appear to be stable in the pelitic schist within the staurolite-aluminum silicate zone. Evidence for metamorphic conditions being at or near the triple point in this zone consists of: (1) the close spatial association of andalusite, kyanite, and sillimanite in the 4 samples in which they occur together; (2) the occurrence of sillimanite and andalusite and sillimanite and kyanite in contact with the same small intervening biotite crystals; (3) the numerous rocks in which combinations of aluminum silicates occur together (of the 10 samples that contain kyanite, all but 2 also have andalusite, and 4 of the 10 have sillimanite); and (4) the absence of any obvious disequilibrium textural relations between polymorphs (with the one exception noted above). The close association between kyanite and andalusite, in which kyanite occurs within and adjacent to a large andalusite grain (fig. 5J), suggests that these two minerals formed during the same metamorphic event. This relation, as well as the presence of a fringe of sillimanite on a few andalusite crystals (see fig. 5J), also suggests that the order of crystallization of aluminum silicates was "normal" with rising temperature at pressures at or slightly below the triple point; kyanite formed first, followed by andalusite and finally by sillimanite. Textural evidence does not appear to indicate a second, lower pressure andalusite-producing event separate from a higher pressure or lower temperature kyanite-producing metamorphic event. Although the discrepancy in geothermometric data from two samples containing all three Al_2SiO_5 polymorphs might suggest possible complexities in thermal history, the good agreement between garnet-biotite equilibration temperatures in the other schist samples in this zone (see table 4 and fig. 6), together with the textural data cited above, argues for equilibrium conditions.

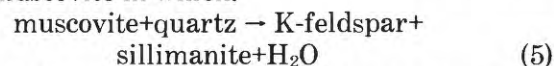
STAUROLITE-OUT ISOGRAD

Whereas the development of sillimanite at the expense of staurolite is not considered to have been significant in pelitic schist within the staurolite-aluminum silicate zone, this reaction was probably very important in the sillimanite gneiss and pelitic schist south of this zone. Staurolite is absent from all samples of sillimanite gneiss and pelitic schist just north of the gneiss, and sillimanite+biotite+garnet is a common assemblage. These mineralogic data have been used to map an isograd, shown on figure 2, on the basis of the disappearance of the staurolite as it is consumed in the sillimanite-producing reaction 4. This isograd defines the north boundary of a zone in which sillimanite and garnet are the key minerals, and for that reason the rocks upgrate of this isograd are here referred to as the sillimanite-garnet zone. The staurolite-out isograd outlines the north and east margin of the proposed gneiss dome.

The common association of sillimanite with biotite in gneiss (fig. 5C) and schist in the sillimanite-garnet zone suggests that some sillimanite formed at the expense of biotite, as has been proposed by several authors in their studies of other areas (Hietanen, 1956, p. 23; Tozer, 1955, p. 313; Woodland, 1963, p. 359, 367; Pitcher and Read, 1963, p. 267, 278). This textural relation could also be explained by a reaction of which biotite is a product, along with sillimanite, rather than a reactant. Thompson and Norton (1968, p. 323) cite reaction 4, discussed above, as one of the reactions which very probably "are responsible for much of the common association of fibrolitic sillimanite with muscovite and biotite."

The absence of staurolite from all samples of pelitic schist and gneiss in the sillimanite-garnet zone is good evidence that reaction 4 accounts for much of the sillimanite present in these rocks. There is no textural evidence in the gneiss of this zone of sillimanite having formed from andalusite, but the occurrence of fringes of sillimanite around grains of andalusite in two equigranular, granitic-appearing rocks may imply that this reaction also took place in the gneiss.

The consistent decrease in muscovite, accompanied by an increase in potassium feldspar in the sillimanite-garnet zone toward the center of the sillimanite gneiss body (fig. 2; table 2), together with the high equilibration temperatures determined for samples of sillimanite gneiss (fig. 6; table 5), indicates that some sillimanite must have formed by the breakdown of muscovite in which:



(reaction 3, Evans, 1965). Because trace amounts of

muscovite are present in most samples of sillimanite gneiss, the breakdown of muscovite appears to be incomplete in most of the rocks, and it has not been possible to map an isograd defined by this reaction.

SILLIMANITE-ANDALUSITE ISOGRAD

The southernmost isograd (fig. 2), which outlines the southwest margin of the proposed dome, has been drawn to pass through two localities in which sillimanite and andalusite coexist in pelitic schist south of the dome, and between two localities, in one of which sillimanite occurs in biotite gneiss north of the isograd and in the other of which andalusite occurs in biotite gneiss south of it. If sillimanite and andalusite are in equilibrium in the rocks in which they both occur, then this isograd may define the area in which the physical conditions of metamorphism were such that the univariant polymorphic reaction andalusite—sillimanite may have occurred.

PROPOSED ORIGIN OF EQUIGRANULAR ALUMINUM SILICATE-BEARING ROCKS

The best explanation of the textural and mineralogical features of the equigranular rocks previously described is that they resulted from synmetamorphic intrusion of small granitic bodies or dikes. Local plutonism may have occurred as the paragneiss was being metamorphosed under the temperature and pressure conditions of the andalusite field. The andalusite and possibly also the garnet grains in these equigranular rocks may represent xenocrysts that were incorporated in a granitic melt that crystallized before the polymorphic transition from andalusite to sillimanite took place in the surrounding paragneiss.

Evidence for a plutonic origin of at least some of the equigranular rocks consists of the oscillatory zoning in plagioclase (fig. 5*F*) observed in several samples, the fact that equigranular rocks crosscut sillimanite gneiss at two localities, and, perhaps, the more perthitic nature of the potassium feldspar relative to sillimanite gneiss in most samples and the presence of myrmekite in several samples.

Evidence that deformation and prograde metamorphism continued subsequent to intrusion of the equigranular rocks consists of the development of crude mineral alignment, incipient cataclastic foliation, and development of some of the sillimanite needles from biotite or andalusite or both (fig. 5*E*). As andalusite was not found in any samples of sillimanite gneiss in the sillimanite-garnet zone in which the equigranular rocks occur, it seems reasonable to conclude that the andalusite grains, presumed to be

xenocrysts, were metastable under sillimanite-grade conditions. The halos of muscovite that rim several grains of andalusite and garnet in two samples could be interpreted as evidence of the instability of andalusite and garnet in the granitic melt. It is not clear whether the granitic melt in any of the areas where equigranular rocks were observed was derived in situ from partial melting of the gneiss or whether the magma was derived at greater depth and injected synmetamorphically. Garnet-biotite equilibration temperatures for the gneiss are high enough to be compatible with partial melting, but the inclusion of andalusite xenocrysts in some of the samples suggests that the granitic rocks were intruded before the peak of metamorphism.

PHYSICAL CONDITIONS OF METAMORPHISM

The mineral assemblages in the pelitic schist and gneiss described in this study are considered to have been produced by a single metamorphic episode, although prior low-grade metamorphic events are not precluded. The only suggestion of prior metamorphic events in the thin sections studied is the partial replacement of garnet by biotite, quartz, muscovite, and feldspar seen in a few samples. This texture might be considered an indication of two prior metamorphic events: one in which garnet was formed, and a subsequent retrograde event in which garnet was replaced. However, because there appears to be no other textural evidence for such previous events and because unreacted and partially replaced garnets occur along with the relict garnets in the same thin section, it seems more likely that this texture resulted from local late-stage retrograde metamorphism. The rare examples of coarse mica flakes lying at an angle to foliation may have grown during the last stages of metamorphism, after major deformation of the rocks.

Experimental phase equilibria pertinent to this study are shown in figure 7. These equilibria, together with the temperatures calculated from the relative distribution of Fe and Mg between coexisting garnet and biotite (table 5), have been used to estimate the range of temperature and pressure conditions that accompanied metamorphism of the pelitic schist and sillimanite gneiss (shown as a stippled pattern in figure 7).

Temperatures of 535° to 600°±30°C obtained from coexisting garnet and biotite in pelitic schist in the staurolite-aluminum silicate zone are consistent with the fact that muscovite and quartz coexist in these samples, whereas K-feldspar is rare (see table 2), and there is no evidence of partial melting of the schist. Staurolite is also present in many of these

samples (table 5). Petrologic data from natural assemblages (Hietanen, 1973; Carmichael, 1978, among others) indicate that the triple point is within the stability field of staurolite in pelitic schist; that conclusion is consistent with our interpretation that andalusite, kyanite, and sillimanite are in equilibrium within the staurolite-aluminum silicate zone. Experimental determination of the upper stability limit of staurolite+quartz (e.g., Richardson, 1968) does not agree with many of the petrologic data reported in the literature and that experimentally determined limit has been shown to be located at implausibly high temperatures (see Thompson, 1976; Carmichael, 1978; Ghent and others, 1979; Hutcheon, 1979; and Ferry, 1980 for discussion of the problems of staurolite equilibrium). For this reason, the experimentally determined staurolite stability field is not shown in figure 7. The temperature range of 535° to $600^{\circ}\pm 30^{\circ}\text{C}$ is based on the rounded averages of temperatures calculated according to Ferry and Spear's calibration (1978). However, use of the equilibration temperatures for pelitic schist calculated from Goldman and Albee's calibration (1977) of 520° to $570^{\circ}\pm 30^{\circ}\text{C}$ (table 4) results in better agreement between the estimated metamorphic temperatures in the schist and the triple-point temperature of about 500°C (Holdaway, 1971).

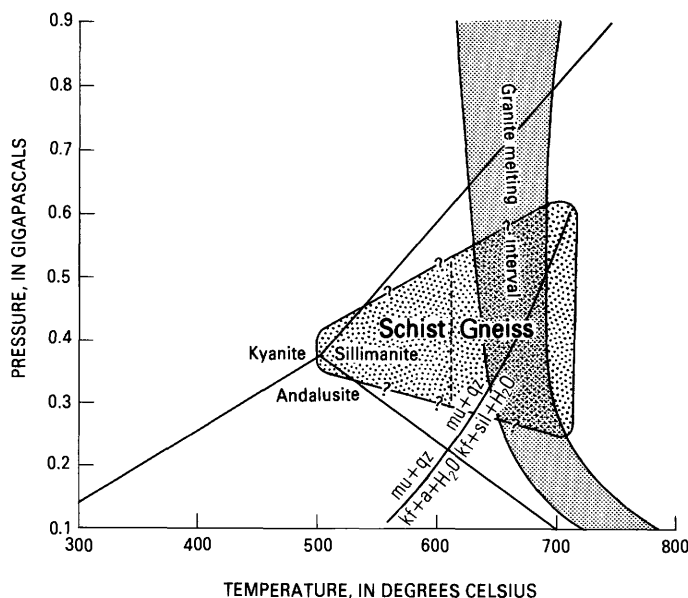


FIGURE 7.—Phase equilibria pertaining to study area. Al_2SiO_5 triple point (Holdaway, 1971); breakdown of muscovite (mu)+quartz (qz) (Chatterjee and Johannes, 1974); melting interval of muscovite granite with excess H_2O (Wyllie, 1977). Best estimate of final pressure and temperature of mineral equilibration in pelitic schist and sillimanite (sil) gneiss shown by stippled pattern. Andalusite (a); k-feldspar (kf).

Pressure during metamorphism of the schist in the staurolite-aluminum silicate zone would be around 0.36 GPa, on the basis of Holdaway's triple point (1971). The absence of kyanite from pelitic schist in the andalusite-sillimanite zone southwest of the proposed dome suggests that pressure conditions may have been slightly less or temperatures slightly greater in this area, relative to conditions in the staurolite-aluminum silicate zone north and east of the gneiss body. The disappearance of andalusite northeast of the andalusite-sillimanite isograd appears to indicate an increase in pressure and (or) temperature conditions northeastward toward the gneiss body, similar to an increase in metamorphic grade toward the gneiss that is documented in pelitic schist north and east of the sillimanite gneiss.

During metamorphism of the sillimanite gneiss, temperature conditions increased toward the center of the body from $655^{\circ}\pm 30^{\circ}\text{C}$ to $705^{\circ}\pm 30^{\circ}\text{C}$. The scarcity of muscovite near the center of the gneiss dome and the ragged appearance of the muscovite, suggestive of instability in rocks in which potassium feldspar is also present, agree with an estimated maximum temperature limit near and probably above that at which the breakdown of muscovite+quartz occurs (Chatterjee and Johannes, 1974). The temperature and mineral-assemblage data, combined with experimental data (fig. 7) and the migmatitic appearance of the gneiss at several localities, suggest that some *in situ* melting of the gneiss may have occurred. Pegmatite and felsic dikes, which are common locally in the gneiss body, are also possible evidence of partial melting.

The pressure during metamorphism of the gneiss body is more difficult to estimate. An upper pressure limit of about 0.8 GPa is required because of the absence of kyanite in all the assemblages. A more reasonable pressure estimate is provided by the combination of the assemblages cordierite+biotite+ Al_2SiO_5 and garnet+biotite+ Al_2SiO_5 , which, according to Hess (1969), suggests a range of 0.3 GPa (at 590°C) to 0.6 GPa (at 710°C). Stability relations of Fe-Mg cordierite with potassium feldspar determined for conditions of muscovite-quartz instability in high-grade pelitic rocks (Holdaway and Lee, 1977) indicate that a pressure range of about 0.2 to 0.5 GPa (depending on the distribution of Fe and Mg between cordierite and biotite and the estimated $P_{\text{H}_2\text{O}}$) corresponds with the temperature range determined for the sillimanite gneiss.

The mineral assemblages that consist of several combinations of the aluminum silicates, staurolite and garnet in the quartz-mica schist are characteristic of the Idahoan-type metamorphic facies series de-

scribed by Hietanen (1967) and the low-pressure intermediate group facies series of Miyashiro (1961). The assemblages sillimanite+orthoclase±muscovite±garnet and sillimanite+cordierite+orthoclase+muscovite in the gneiss are also compatible with those facies series.

CONCLUSIONS

The possibility that the sillimanite gneiss body is a gneiss dome was previously postulated (Foster and others, 1977b) on the basis of mapped relations, such as the distribution of high-grade metamorphic rocks. The petrography and geothermometry presented in this paper support the gneiss dome hypothesis. Evidence that the large body of sillimanite gneiss and schist (between the staurolite-out and andalusite-sillimanite isograds) is a gneiss dome consists of the following: (1) the topographic expression of a circular area with a radial drainage pattern, (2) the general outward dip of foliation (see fig. 2), (3) the increase in metamorphic grade from a staurolite-aluminum silicate zone on the north and east and possibly an andalusite sillimanite zone on the southwest to a sillimanite-garnet zone (fig. 2) and the breakdown of muscovite+quartz in the central part of the body, and (4) the increase in equilibration temperatures from those for pelitic schist flanking the proposed dome (535° to $600^{\circ}\pm 30^{\circ}\text{C}$) to those for sillimanite gneiss in its core ($705^{\circ}\pm 30^{\circ}\text{C}$).

The distribution of key minerals and of equilibration temperatures, calculated on the basis of the relative distribution of Fe and Mg between biotite and garnet in pelitic schist and sillimanite gneiss, indicates an increase in metamorphic temperature from the flanks of the proposed gneiss dome to its core. Pelitic schist that flanks the gneiss on the north and east equilibrated at temperatures in the range of about 500° to 630°C . Locally, metamorphic conditions were probably close to those under which all three aluminum silicates are stable. Rocks composing the gneiss dome equilibrated at temperatures in the range of about 650° to possibly as much as 730°C . Partial melting of the pelitic rocks in the center of the dome may have occurred locally. Synmetamorphic intrusion of equigranular aluminum-silicate-bearing rocks probably took place while metamorphic conditions were in the temperature-pressure field for the formation of andalusite as the stable aluminum silicate polymorph.

Throughout much of the gneiss dome, the sillimanite gneiss is not truly migmatitic; this, on the basis of comparison with some gneiss domes in the Shuswap Metamorphic Complex of British Columbia

(Reesor, 1970), could imply that deep structural levels of the gneiss dome core are not exposed. The apparent gradual transition from sillimanite gneiss to pelitic schist on the north and east also suggests that the sillimanite gneiss represents a fairly high structural level of the dome and may be composed wholly or in part of mantling rocks.

The relationship of the greenschist facies rocks to the pelitic schist that flanks the sillimanite gneiss on the north and east is probably that of a thrust fault. North of the dome, pelitic schist is separated from greenschist facies rocks by a zone of cataclastic rocks, and regional relations suggest that the thrusting is probably not directly related to the rise of the gneiss dome.

Other gneiss domes may be present in the Yukon crystalline terrane. For instance, an unstudied area about 60 km northeast of the sillimanite gneiss dome, of topographically high amphibolite facies gneiss and schist, may have a domal structure. At present, the sillimanite gneiss dome cannot be related definitely to structural trends or thermal patterns in the Yukon crystalline terrane. However, the fact that the gneiss dome occurs on line with the general trend of augen gneiss batholiths in east-central Alaska and Yukon Territory suggests the possibility that metamorphism of the gneiss dome and intrusion of augen gneiss occurred in response to the same set of thermal and tectonic conditions. This genetic relationship is also suggested by U-Pb isotopic studies that indicate a Mississippian intrusive age for the augen gneiss batholith southeast of the gneiss dome (Aleinikoff and others, 1981a) and a possible, albeit poorly constrained, Mississippian metamorphic age for the gneiss dome (Aleinikoff and others, 1983a). Further study of the para- and ortho-gneisses in the Yukon crystalline terrane is necessary in order to evaluate the significance of the general trend defined by the augen gneiss batholiths and to better understand the structural and thermal history of this terrane.

REFERENCES CITED

- Aleinikoff, J. N., Dusel-Bacon, Cynthia, and Foster, H. L., 1981a, Geochronologic studies in the Yukon-Tanana upland, east-central Alaska, in Albert, N. R. D., and Hudson, Travis, eds., *The United States Geological Survey in Alaska: Accomplishments during 1979*: U.S. Geological Survey Circular 823-B, p. B34-B37.
- Aleinikoff, J. N., Dusel-Bacon, Cynthia, Foster, H. L., and Futa, Kiyoto, 1981b, Proterozoic zircon from augen gneiss, Yukon-Tanana Upland, east-central Alaska: *Geology*, v. 9, no. 10, p. 469-473.
- Aleinikoff, J. N., Dusel-Bacon, Cynthia, and Foster, H. L., 1983a, Uranium-lead isotopic ages of zircon from sillimanite gneiss and implications for Paleozoic metamorphism, Big Delta

- quadrangle, east-central Alaska, *in* Coonrad, W. L., and Elliott, R. L., eds., *The United States Geological Survey in Alaska: Accomplishments during 1981: U.S. Geological Survey Circular 868* [in press].
- Aleinikoff, J. N., Foster, H. L., Nokleberg, W. J., and Dusel-Bacon, Cynthia, 1983b, Isotopic evidence from detrital zircons for Early Proterozoic crustal material, east-central Alaska, *in* Coonrad, W. L., and Elliott, R. L., eds., *The United States Geological Survey in Alaska: Accomplishments during 1981: U.S. Geological Survey Circular 868* [in press].
- Baltatzis, E., 1979, Distribution of Fe and Mg between garnet and biotite in Scottish Barrovian metamorphic zones: *Mineralogical Magazine*, v. 43, no. 325, p. 155-157.
- Carmichael, D. M., 1978, Metamorphic bathozones and bathograds: a measure of the depth of post-metamorphic uplift and erosion on the regional scale: *American Journal of Science*, v. 278, no. 6, p. 769-797.
- Chatterjee, N. D., and Johannes, Wilhelm, 1974, Thermal stability and standard thermodynamic properties of synthetic 2M₁-muscovite, KAl₂(AlSi₃O₁₀(OH)₂): *Contributions to Mineralogy and Petrology*, v. 48, no. 2, p. 89-114.
- Churkin, Michael, Jr., Foster, H. L., Chapman, R. M., and Weber, F. R., 1982, Terranes and suture zones in east central Alaska: *Journal of Geophysical Research*, v. 87, no. B5, p. 3718-3730.
- Evans, B. W., 1965, Application of a reaction-rate method to the breakdown equilibria of muscovite and muscovite plus quartz: *American Journal of Science*, v. 263, no. 8, p. 647-667.
- Ferry, J. M., 1980, A comparative study of geothermometers and geobarometers in pelitic schists from south-central Maine: *American Mineralogist*, v. 65, no. 7-8, p. 720-732.
- Ferry, J. M., and Spear, F. S., 1978, Experimental calibration of the partitioning of Fe and Mg between biotite and garnet: *Contributions to Mineralogy and Petrology*, v. 66, no. 2, p. 113-117.
- Foster, H. L., 1970, Reconnaissance geologic map of the Tanacross quadrangle, Alaska: U.S. Geological Survey Miscellaneous Geologic Investigations Map I-593, 1 sheet, scale 1:250,000.
- Foster, H. L., 1976, Geologic map of the Eagle quadrangle, Alaska: U.S. Geological Survey Miscellaneous Investigations Series Map I-922, scale 1:250,000.
- Foster, H. L., Albert, N. R. D., Griscom, Andrew, Hessin, T. D., Menzie, W. D., Turner, D. L., and Wilson, F. H., 1979, *The Alaskan Mineral Resource Assessment Program: Background information to accompany folio of geologic and mineral resource maps of the Big Delta quadrangle, Alaska: U.S. Geological Survey Circular 783*, 19 p.
- Foster, H. L., Dusel-Bacon, Cynthia, and Weber, F. R., 1977a, Reconnaissance geologic map of the Big Delta C-4 quadrangle, Alaska: U.S. Geological Survey Open-File Report 77-262, scale 1:63,360.
- Foster, H. L., and Keith, T. E. C., 1974, Ultramafic rocks of the Eagle quadrangle, east-central Alaska: U.S. Geological Survey *Journal of Research*, v. 2, no. 6, p. 657-669.
- Foster, H. L., Weber, F. R., and Dusel-Bacon, Cynthia, 1977b, Gneiss dome in the Big Delta C-4 quadrangle, Yukon-Tanana Upland, Alaska, *in* Blean, K. M., ed., *The United States Geological Survey in Alaska: Accomplishments during 1976: U.S. Geological Survey Circular 751-B*, p. B33.
- Ghent, E. D., Robbins, D. B., and Stout, M. Z., 1979, Geothermometry, geobarometry, and fluid compositions of metamorphosed calc-silicates and pelites, Mica Creek, British Columbia: *American Mineralogist*, v. 64, no. 7-8, p. 874-885.
- Goldman, D.S., and Albee, A. L., 1977, Correlation of Mg/Fe partitioning between garnet and biotite with ¹⁸O/¹⁶O partitioning between quartz and magnetite: *American Journal of Science*, v. 277, no. 6, p. 750-767.
- Hess, P. C., 1969, The metamorphic paragenesis of cordierite in pelitic rocks: *Contributions to Mineralogy and Petrology*, v. 24, no. 3, p. 191-207.
- Hietanen, Anna, 1956, Kyanite, andalusite, and sillimanite in the schist in Boehls Butte quadrangle, Idaho: *American Mineralogist*, v. 41, no. 1-2, p. 1-27.
- 1967, On the facies series in various types of metamorphism: *Journal of Geology*, v. 75, no. 2, p. 187-214.
- 1973, *Geology of the Pulga and Bucks Lake Quadrangles, Butte and Plumas Counties, California: U.S. Geological Survey Professional Paper 731*, 66 p.
- Holdaway, M. J., 1971, Stability of andalusite and the aluminum silicate phase diagram: *American Journal of Science*, v. 271, no. 2, p. 97-131.
- Holdaway, M. J., and Lee, S. M., 1977, Fe-Mg cordierite stability in high-grade pelitic rocks based on experimental, theoretical and natural observations: *Contributions to Mineralogy and Petrology*, v. 63, no. 2, p. 175-198.
- Hutcheon, I., 1979, Sulfide-oxide-silicate equilibria; Snow Lake, Manitoba: *American Journal of Science*, v. 279, no. 6, p. 643-665.
- Labotka, T. C., 1980, Petrology of a medium-pressure regional metamorphic terrane, Funeral Mountains, California: *American Mineralogist*, v. 65, no. 7-8, p. 670-689.
- Mason, Brian, 1966, *Principles of Geochemistry*: New York, John Wiley and Sons, Inc., 329 p.
- Mertie, J. B., 1937, *The Yukon-Tanana region, Alaska: U.S. Geological Survey Bulletin 872*, 276 p.
- Misch, Peter, 1971, Porphyroblasts and "crystallization force": Some textural criteria: *Geological Society of America Bulletin*, v. 82, no. 1, p. 245-252.
- Miyashiro, Akiho, 1961, Evolution of metamorphic belts: *Journal of Petrology*, v. 2, no. 3, p. 277-311.
- Pitcher, W. S., and Read, H. H., 1963, Contact metamorphism in relation to manner of emplacement of the granites of Donegal, Ireland: *Journal of Geology*, v. 71, no. 3, p. 261-306.
- Reesor, J. E., 1970, Some aspects of structural evolution and regional setting in part of the Shuswap metamorphic complex: *Geological Association of Canada Special Paper 6*, p. 73-86.
- Richardson, S. W., 1968, Staurolite stability in a part of the system Fe-Al-Si-O-H: *Journal of Petrology*, v. 9, no. 3, p. 467-488.
- Spry, Alan, 1969, *Metamorphic textures*: New York, Pergamon Press, 350 p.
- Tempelman-Kluit, D. J., 1976, The Yukon crystalline terrane: Enigma in the Canadian Cordillera: *Geological Society of America Bulletin*, v. 87, no. 9, p. 1343-1357.
- Tempelman-Kluit, Dirk, and Wanless, R. K., 1980, Zircon ages for the Pelly Gneiss and Klotassin granodiorite in western Yukon: *Canadian Journal of Earth Sciences*, v. 17, no. 3, p. 297-306.
- Thompson, A. B., 1976, Mineral reactions in pelitic rocks: II. Calculation of some P-T-X (Fe-Mg) phase relations: *American Journal of Science*, v. 276, no. 4, p. 425-454.
- Thompson, J. B., and Norton, S. A., 1968, Paleozoic regional metamorphism in New England and adjacent areas, *in* Zen, E-An, White, W. S., and Hadley, J. B., eds., *Studies of Appalachian Geology: Northern and Maritime*: New York, John Wiley, p. 319-327.
- Tozer, C. F., 1955, The mode of occurrence of sillimanite in the Glen District, Co. Donegal: *Geological Magazine*, v. 92, no. 4, p. 310-320.
- Weber, F. R., Foster, H. L., Keith, T. E. C., and Dusel-Bacon, Cynthia, 1978, Preliminary geologic map of the Big Delta quadrangle, Alaska: U.S. Geological Survey Open-File Report 78-529-A, scale 1:250,000.
- Woodland, B. G., 1963, A petrographic study of thermally meta-

- morphosed pelitic rocks in the Burke area, northeastern Vermont: *American Journal of Science*, v. 261, no. 4, p. 354-375.
- Wyllie, P.J., 1977, Crustal anatexis: an experimental review: *Tectonophysics*, v. 43, nos. 1-2, p. 41-71.
- Yakowitz, H., Myklebust, R. L., and Heinrich, K. F. J., 1973, FRAME: An on-line correction procedure for quantitative electron probe analysis: National Bureau of Standards Technical Note 796, 46 p.

